AN ACOUSTICAL BASED APPROACH TO CONCEPTUAL DESIGN OF NON-TRADITIONAL ROTORCRAFT CONFIGURATIONS

A Thesis
Presented to
The Academic Faculty

By

Sara A. Huelsman

In Partial Fulfillment
of the Requirements for the Degree
Master of Science in the
School of Aerospace Engineering

Georgia Institute of Technology

August 2020

AN ACOUSTICAL BASED APPROACH TO CONCEPTUAL DESIGN OF NON-TRADITIONAL ROTORCRAFT CONFIGURATIONS

Approved by:

Dr. Mavris, Advisor
School of Aerospace Engineering
Georgia Institute of Technology

Dr. Elena Garcia
School of Aerospace Engineering
Georgia Institute of Technology

Mr. Busch
School of Aerospace Engineering
Georgia Institute of Technology

Date Approved: July 15, 2020

The hammer never complains of the noise

Marty Rubin

I would like to dedicate this thesis to new beginnings, especially after so many new beginnings, to sunrises and sunsets in Atlanta, to the city skyline, to always getting up and trying again, to diversity, to community, to poetry, to open mics, to never ending sentences, and to all the love that commas cant contain.

I would like to dedicate this thesis to consistency, to studying, to routine, to going to the gym, to going to poetry, to roots, to Wisconsin, to foundation, to always having these to fall back on when things get rough, to unconditional love wherever you get it, to my cat Oreo, to tenacity, to strength and to creating these when you feel you have none.

To science, to art, to sound, whether it be danger or safety, and to my ears for still learning the difference.

ACKNOWLEDGEMENTS

I would like to acknowledge Dr. Dimitri Mavris for accepting me into Georgia Institute of Technology, but also funding me during my time here, and being flexible with my academic needs. I would like to thank Elena Garcia for being on my committee for my thesis.

My gratitude also goes towards Greg Busch for spending his spare free hours guiding me through this thesis and always believing in my ability. Thank you for showing me I can make it in engineering.

I would like to thank SAFRAN for providing the motivation and funding for this research.

TABLE OF CONTENTS

LIST OF TABLES

LIST OF FIGURES

NOMENCLATURE

c speed of sound

ΔSPL_K correction factor for rotors with different c/D

M_{dd} drag divergence Mach number

ΔSPL_C normalized compressibility-induced profile drag noise component

T total system thrust

c_0 speed of sound at standard sea level conditions

ρ density

ΔSPL_{mr} normalized main rotor noise component sound pressure level

L_0 blade lift

N rotational speed

$\bar{C_L}$ lift coefficient

β observer angle measured from rotor disk plane

ΔSPL_{bv} blade-vortex interaction noise component sound pressure level

$SPL_{1/3}$ one-third octave band sound pressure level

V_T blade tip speed

A_b blade area

$S_{1/3}$ normalized broadband noise spectrum

η rotating system of axes

η_1 parallel to the chord of a blade

τ source time

Ω angular velocity

$SPL_{m\beta}$ sound pressure level at a given harmonic frequency

θ	outward normal to the body and $\overrightarrow{r}$
F	thickness function of the airfoil
Γ	curve of intersection of blade surface
v	helicopter speed
$\overrightarrow{r}$	a vector from the origin of the xyz frame to the field point
φ	angle between $\overrightarrow{r}$ and the z axis
c_0	speed of sound in undisturbed surroundings
S_2	total surface area of rear rotor blades
t	observer time
$\Box$	d'Alembert operator
M_e	effective tip Mach number
T_{ij}	Lighthill stress tensor
f	flow fluid
u_n	fluid velocity in direction normal to the surface f = 0
v_n	surface velocity in direction normal to the surface
M_n	v_n/c
p'	acoustic pressure
$H(f)$	Heaviside function
$\partial(f)$	the Dirac delta function
R	rotor radius
r	distance from source to observer
B	number of blades
h	blade thickness
c	blade chord length

SUMMARY

As interstate and highway traffic increases commute times become drastically large. Such large commute times create fatigue and take away from productive hours at work, or joyful hours at home. The idea of urban air mobility becomes increasingly more attractive and viable as technology improves. These more advanced rotor concepts have opened up the design space in order to satisfy a very different mission profile. Nontraditional rotor concepts can provide performance benefits within a new use of the design. Designers have been exploring various new configurations that there is not much research behind.

In the past, since rotors have been used in a traditional helicopter configuration, acoustic research is centered around this configuration. Through this history, aspects of these UAM configurations can be extrapolated. Rotors generate a diverse spectrum due to the many noise sources. Each of the noise types have been matched up with their respective sources and discussed. Rotor noise is separated into periodic noise or harmonic and non periodic noise, which depend on rotor noise source whether it is sourced from the circling of the blade or random fluctuations. Thickness noise is generated from the thickness of the airfoil blade, loading noise is generated from the loading on the blade, and broadband noise accounts for all random turbulent fluctuations. These noise types have various levels of fidelities they can be modeled within; semi-empirical, analytical, and numerical. This thesis summarizes rotorcraft acoustic principles and modeling techniques in various fidelities.

Previous research primarily focused on source noise identification which provides some of the possible design parameters that can influence noise. By looking at configurations that can build off each other, along with these design parameters that can impact noise, run matrices can be generated. This thesis looks at coaxial rotors, a ducted rotor, and a combination of both with a ducted coaxial rotor system. The run matrices are divided into configuration parameters and design parameters, as to section the potential noise generators. This way it can be seen if the noise can be contained through the configurations or the

rotor design alone.

Since these urban air mobility vehicles are flying in close proximity to people and buildings, noise becomes a larger concern, but there is not a lot of research at how an acoustic signature might change due to configuration. There is a particular literature gap for acoustic modeling within the conceptual design stage for advanced configurations. This thesis aims to help create an approach for designing these configurations with acoustic concerns.

By using a higher fidelity numerical model and varying design and configuration parameters, influential parameters of rotorcraft acoustics can be identified. If trends can be identified from these parameters and their corresponding outputs, a lower fidelity model may be generated in order to represent an acoustic signature of an advanced rotor concept at the conceptual design stage.

This research presents the results from detailed noise modeling, analyzes trends within the results, and fits a model to the data. This best fit model provides a simplified way of accurately accounting for noise early on in the design stages. Such a model demonstrates the ability to design with noise in mind, for a new class of vehicles. Additionally, it gives insight on what level of CFD fidelity is necessary for acceptable noise results, and source noise generation and non-traditional rotorcraft configurations. While the aerodynamic analysis was not the main objective of this thesis, the CFD was substantiated and assured to be acceptable through multiple ways. The flight conditions for these rotary systems were taken from Schatzman's work as to confirm authenticity in comparison and how noise may change in similar situations [1]. A sensitivity study for mesh size was not done as to save computational time, but the results were accepted in accordance to the convergence of the residuals. Mach number contours matched the desired input as well as the shape match that of Schatzman's. The surface pressures were exported into an acoustic solver for further analysis.

PSU-WOPWOP was the acoustic solver used for this research which uses Ffwocs

Williams Hawking's Equation. This is an extension of Lighthill's acoustic analysis, and allows for the design sources to be separated and summed. The direct noise source in reference to the specific vehicle design can be isolated. PSU-WOPWOP accomplishes this all by taking in geometry and surface pressures. Geometry file is representative of a single blade and generated by predetermined parameters along defined span locations. The blade is then repeated as needed for the case. Loading files are generated using the surface pressures from CFD and converted into forces, which are then distributed across the revolution of the blade spinning.

Representative models provide ways in which equations can fit the data, and therefore substitute the process to provide accurate acoustic data within an earlier design stage. This representative model is the final output of this thesis. Multiple representative models were attempted including neural networks, fit of least squares, and stepwise regression. The best fitting model was determined through a small standard deviation, no outliers, and an R squared close to one. Other important graphs that assisted in determining the best fitting model was residual by predicted plots, and actual by predicted plots that displayed a good spread of the data and lack of outliers.

The acoustic results show consistency across all configurations. The frequency shows that thickness noise is the primary source. Looking at the influential parameter results from predictor screenings, coaxial rotors show that majority of noise is generated from design parameters. The configuration parameters are less influential. Within the ducted cases it remains consistent that the design parameters are more significant and the configuration parameters are less. The ducted coaxial configuration displays a similar pattern with more significant design parameters than configuration parameters. Across all three configurations the most influential parameters were blade tip Mach number, chord, and rotor radius. This confirms the physics relationship between noise and sound. Thickness noise being a primary source, substantiates the chord length being a large driver of noise. Finally, rotor radius showed to have an inverse relationship to noise, showing that a larger rotor radius

allowed for less turbulence and noise.

The best fitting model was the stepwise regression model which displayed similar trends throughout the configurations. These trends showed that a simplified model can be created to capture rotor noise through rotor design and configuration parameters. This shows that noise trends can be accounted for in an early design stage for UAM design spaces of interest.

CHAPTER 1

INTRODUCTION AND BACKGROUND

1.1 Introduction and Motivation

As city population increases so do commute times. This takes away from important hours at work or at home and creates fatigue. While roadways are clogged, the airways remain open for exploration. This generates a very different mission profile for flight vehicles.

Flight has traditionally been used for longer travel where landing can take place further away from residents. Urban air mobility creates the concept of a shorter mission profile to travel from home to work with landing and takeoff being amongst homes or work life. Due to the landing and takeoff happening in such close proximity to buildings and the need to conserve space, vertical take-off and landing is the most rational method of transport.

More advanced concepts and configurations are being explored due to their potential benefits. Many provide performance advantages such as increased lift or thrust, or reduced sized rotors. These benefits are especially helpful when designing UAM vehicles due to the different mission profile. UAM vehicles are flying in more confined spaces, such as cities, and space limitations become more prevalent[2].

Rotary concepts have been known to be noisy which remains one of their main drawbacks. While urban air mobility has these vehicles flying much closer to people than traditional aircraft, they have been shown to be quieter than traditional helicopters. The Volocopter has been shown to have at least a ten decibel drop compared to the R22, as well as a very different acoustic signature [3]. With the various differences between urban air mobility and traditional rotorcraft flight, a method to capture a representative sound within the conceptual design stage needs to be created.

Noise is an important aspect to consider when introducing these vehicles to the com-

munity because they cannot be integrated into everyday life without community acceptance [4]. A history of rotorcraft noise, along with computational modeling efforts of this noise is detailed in this thesis. Additionally, current literature gaps are highlighted, and a potential approach to address them is provided.

1.2 Background

UAM vehicles tend to be smaller than traditional helicopters. Usually, UAM vehicles seat one or two people while traditional helicopters can seat four. This is because they want a smaller payload for UAM vehicles so they can move more quickly and efficiently. Current modeling tools are only valid for larger vehicles that seat more than two people[4].

1.2.1 Acoustics and Noise Types

It is important to fully understand the problem of interest. Therefore, noise must be understood in its generation (source). Many noise types can be produced from a rotorcraft design. Discussed below are the creation and characteristics of thickness, loading, broadband, Blade Vortex Interaction (BVI), and High-Speed Impulse (HSI).

Noise sources are defined by how the noise propagates from them. This is important to note because rotorcraft acoustics tend to be very directional. If noise propagates equally in all directions, spherically, it is a monopole noise source. See Figure 1.1. A dipole noise source is one in which noise only propagates in two equally, but opposite directions. Meaning that there is only noise heard 180 degrees apart from the two directions and no noise is heard in the other directions. See Figure 1.2. A noise source that propagates in four directions equally is a quadrupole. See Figure 1.3 [5].

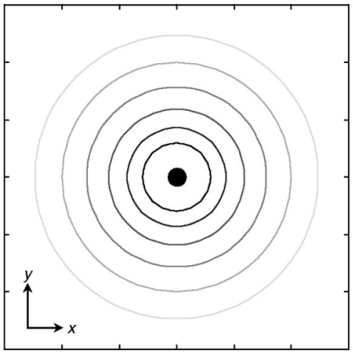

Figure 1.1: A monopole sound source [6]

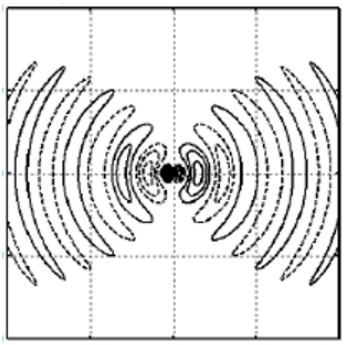

Figure 1.2: A dipole sound source [7]

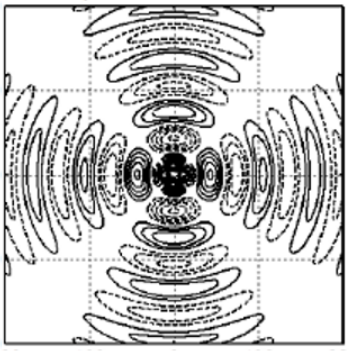

Figure 1.3: A quadrupole sound source [7]

The sound that is produced by these noise sources is typically separated into two categories, tonal noise or broadband noise, which add up to the total noise. Tonal noise is harmonic in nature. Broadband noise is due to random fluctuations of loading or aerodynamic phenomena. Broadband noise is harder to describe because of the random nature, while tonal noise are distinct tones and are more likely from cyclic sources. The following are a list of noise types defined and grouped commonly in literature.

1.2.1 Thickness Noise

Thickness noise is the noise produced by the thickness of the rotor blade cutting through the air. It is generally harmonic in nature due to the rotational nature of the blades. This noise type produces a monopole source, which acts spherically in all directions [5]. Due to the source coming from the blade, thickness noise tends to propagate along the plane of the rotor. This can make the directivity act more in the plane of the rotor and less directly underneath the rotor. In previous studies, it is shown that thickness noise can go to zero directly underneath the rotor[1]. This noise type is the easiest to model as a geometry and motion is all that is required regardless of modeling type [8, 9, 10, 11].

When the blade tip speed begins to enter the supersonic regime, thickness noise begins to increase to a point where it creates a different noise type called HSI [5].This generates a quadrupole type source that can be very complicated to model, but can be easily avoided

by staying within a subsonic regime.

1.2.1 Loading Noise

The noise produced from the loading on the blade is referred to as the loading noise. This force can be fluctuating or steady and the noise will reflect that. Loading noise is a dipole noise source and acts below and above the rotor [5]. Typically, any noise that propagates above the rotor is ignored because it would dissipate into the atmosphere.

At high speeds, the vortices shed off the blade in close enough proximity that the vortices begin to interact. This generates a different noise type called BVI. This is a quadrupole noise source that has directionality forward, behind and/or under the rotor. The other noise direction acts above the rotor and is often ignored because it would not propagate to the ground where receivers would be. BVI is the unsteady pressure fluctuations on a blade caused by interactions with previously generated tip vortices [5] [11]. This noise has been correlated to flight condition and miss distance, which is the vertical distance between the shed vortex and rotor plane. In order to minimize BVI, one would look to minimize miss distance.

1.2.1 Broadband Noise

Broadband noise is the production of many different noise sources that generate the same type of noise. Blade loading associated with turbulent flow on or near the blade surface is the source of broadband noise [5].

This means that broadband noise includes noise generated by turbulence ingestion noise, Blade Wake Interaction (BWI), and blade self-noise. Turbulence ingestion noise happens because of atmospheric turbulence and wake re-circulation that occurs near the ground. High or low frequency can be produced depending on the eddy size. BWI occurs when the rotor encounters wake turbulence and produces mid frequency noise. This produces a significant amount of fluctuating inflow velocity, which effects performances dur-

ing forward flight or climb. Blade self-noise can be produced by several different sources. Boundary layer turbulence, separated boundary layer, vortex shedding, and tip vortex formation are just some of the possible aerodynamic properties that can cause blade self-noise [5].

Broadband noise falls in a frequency range that is very sensitive to the human ear (1 to 5kHz) [12]. This can make this noise type very important to model, while the modeling associated with broadband noise can be rather complicated.

1.2.2 Flight Condition Influence on Acoustics

All of these different noise types create the acoustic signature of a vehicle. As the vehicle moves along its mission profile, particular noise types can become more dominate than others. This is important to note so that the dominate noise type is not only included, but the primary focus. Meaning that if a more complex noise type is dominate, a certain level of fidelity might be required in order to accurately represent that noise type. Dominate noise types can also be used to determine if other noise types are negligible, if so, modeling can be potentially simplified [5].

Since a rotorcraft will always have thickness to its blades and loading on the blades, thickness and loading noise remain important contributors to the acoustic signature throughout the mission profile. As a traditional helicopter ascends and descends, broadband and BVI noise dominate the acoustic signature. Broadband remains dominate throughout forward flight. If the vehicle were to enter high speed forward flight than HSI noise would dominate accordingly. As far as how the acoustic signature of non traditional rotorcraft vehicles would change throughout a mission profile is an area of research that is underdeveloped. For now, it is assumed that non traditional vehicles follow a similar enough pattern to a traditional helicopter [5].

1.2.3 Configuration

Most often designers use different configurations than a traditional isolated rotor for the performance benefits. It is shown that configurations such as a ducted rotor can provide similar thrust with a smaller rotor [13]. This can be useful when designing for UAM vehicles space limitations. A coaxial rotor allows for the elimination of a tail rotor or other anti-torque control along with the potential for greater lift efficiency [14]. UAM vehicles can especially take advantage of this benefit due to a simplified design and physical space limitations.

All of these different noise types are apparent with any type of rotorcraft, but the acoustic signature changes based on configuration. It is important to note conceptually how configuration influences noise, in order to quantify this information later.

1.2.3 Ducted Rotors

When looking at ducted rotors in comparison to an open rotor, the duct shields noise in the plane of the rotor. Since thickness noise is generated from the thickness of the blade, thickness noise is reduced greatly due to the blockage of the duct. The duct also takes some of the loading off the blade and therefore loading noise is also reduced. Broadband noise increases though due to the boundary layer turbulence between the blades and the wall of the duct [13].

The duct dimensions are highly influential on the acoustic signature. While the thicker the duct the less noise is transmitted through it and more is shielded, the length of the duct can possibly hinder the design. Ducted rotors can be louder at higher frequencies depending on if resonance of the duct occurs, this is controlled by the length of the duct matching the wavelength of the frequency. This can be avoided by ensuring that the Blade Passage Frequency (BPF) of the rotor does not reach the resonant frequency, which would be controlled through the RPM of the rotor. It has been shown that a ducted rotor can be overall slightly louder than an isolated rotor, but they are relatively close in magnitude

[15]. Due to the increase in boundary layer turbulence and complex nature of the noise generated, CFD is recommended when analyzing this type of configuration [13].

1.2.3 Coaxial Rotors

Coaxial rotors refers to a rotor system with two sets of blades vertically distributed from each other on the same hub and motor. These blades rotate in opposite directions from each other. This means there are twice as many blades as the traditional main helicopter rotor, which means higher thickness noise. If this configuration is run in supersonic conditions, where HSI noise would occur, HSI noise would be much greater than traditional helicopter HSI noise. This is due to the shock rotor blade interaction between the upper and lower rotors. Due to unsteady loading on coaxial blades, the loading noise increases in this configuration. Since BVI noise is an extension of loading noise, this means that BVI noise would also increase due to more vortices and more blades interacting. Broadband noise would also increase due to the increase in vortices and unsteady nature of this configuration [1, 14].

The most influential parameter within this configuration is the vertical separation between the blades. This particular parameter has an interesting effect on the acoustic signature. While reducing the axial gap between the rotors reduces the broadband noise component it increases the tonal component. This gives the impression that there is some optimal axial gap that can be calculated, but research within this area is limited. Due to the increase in air circulation and complex nature of the noise generated, CFD is recommended when analyzing this type of configuration [1].

*1.2.3 Ducted Coaxial (*Both*) Rotors*

A ducted coaxial rotor configuration is an interesting hybrid of the previous mentioned configurations. Since this configuration is a combination of the previous two, it will be referenced as "*both*" for now. No research was found about this particular configuration in

terms of acoustics.

It is assumed that this particular configuration would potentially act in a combined fashion as the two individually would. While the two rotors would create more thickness noise, the duct would shield noise in the plane of the rotor, and the thicker the duct, the more shielding. The length of the duct could still create resonance that would need to be avoided. Loading noise would be less than an open coaxial rotor due to the duct taking some of the loading, but greater than a single ducted rotor. This configuration possibly falls in between the aforementioned configurations, being generally louder than a ducted rotor, but less than an open coaxial rotor. This is all assumed and many factors can change or influence this estimation such as various design parameters, flight condition, and directionality.

1.2.4 Modeling

Acoustic modeling generally has two parts, the surface pressures on the object or system in question (usually calculated through CFD), and the propagation to a receiver. This allows separation between the system and the environment the system is in. Lower fidelity models would combine the two processes into one equation for simplicity and speed. Higher fidelity models keep the two processes separate.

There are many different ways to model noise with varying degrees of accuracy. Usually the simpler the model (i.e. less computational time and fewer inputs), the higher the degree of uncertainty. These various types of modeling, even those with a higher degree of accuracy, can still be useful within the early design stages. Several different models of varying degrees of accuracy and inputs were surveyed.

The main interest of this project was a model to be used in the conceptual design stage that had few inputs, fast computational time, with the drawback of having higher uncertainty in the results.

The following documents the various modeling types that were looked at, which include semi-empirical and numerical models.

1.2.4 Semi-Empirical

Empirical models are based off of experimentation, tend to be less timely, and are best used in a preliminary design state due to the low number of inputs required. They tend to have a lower fidelity compared to numerical models with many assumptions and with this type of modeling, each noise type is calculated as an isolated noise source and in order to have a full acoustic signature of the rotorcraft, the calculations would have to be for each noise type, summed across noise types and then repeated for various distances and frequencies. It is important to expand across these dimensions in situations where a high frequency may return a low noise level, while a low frequency may return a high noise level. Refusing to look at the many dimensions of noise, may allow for certain parameters to be overlooked. This would result in improper design in accordance to noise and annoyance from the community. There is potential for this to be bypassed by looking at particular frequency bands where noise for these vehicles tend to be the highest.

Even with this repetition, the time of calculations would be less costly compared to numerical models [16]. Figure 1.4 shows how rotor noise can be divided down into individual parts to be modeled separately. While Figure 1.5 displays the steps one would go about to use all the models in conjunction with each other.

1.2.4.1.1 Thickness Noise Thickness noise can be easily modeled with very few inputs using the work of Hawkings and Lowson. In this model, the geometry of the blade matters fairly little since it only requires the number of blades, the chord length, and the blade thickness. It is assumed that the blade chord to rotor diameter ratio value is .03 due to commonality in original designs. The incremental sound pressure level adjustment, which is another input parameter is a correction factor which corrects for rotors with different blade chord to rotor diameter ratio values [16]. For other design conditions the effective tip Mach number is needed, as well as receiver location. This is very minimum information about how fast the vehicle is flying from where. Other computational processes would

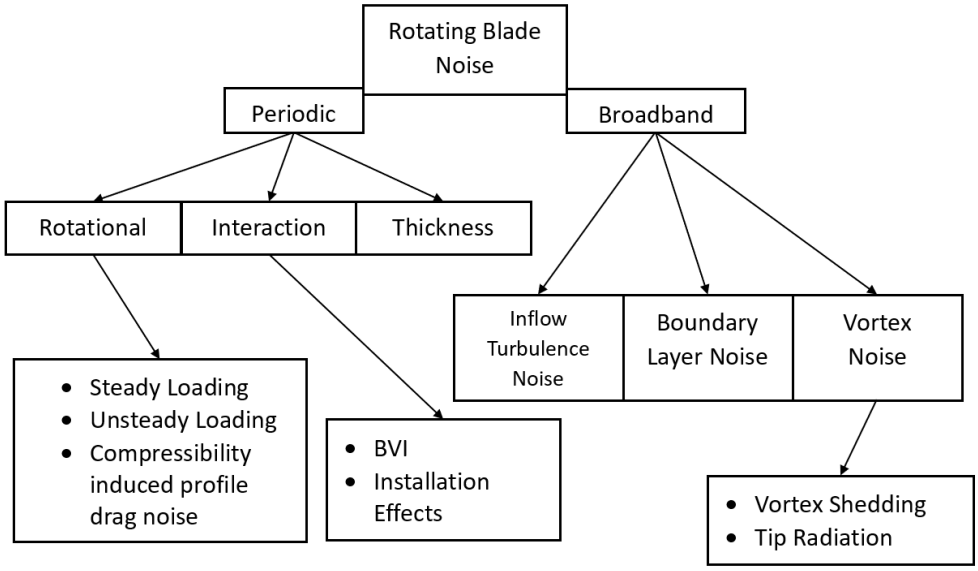

Figure 1.4: Flowchart for the various semi-empirical rotorcraft models (recreated from [16])

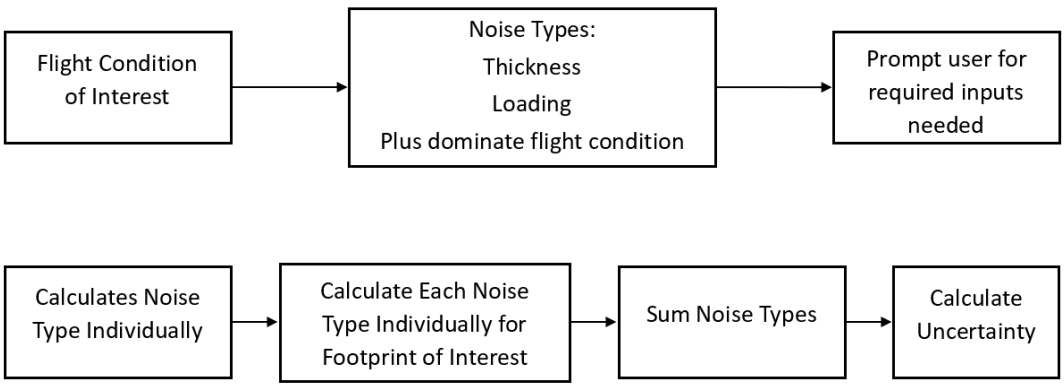

Figure 1.5: Flowchart that shows how the aforementioned semi-empirical models would be used generically

require most information.

Equation 1.1 computes the sound pressure level at a given harmonic frequency. In order to acquire a full spectrum of frequencies the equation would have to be repeated numerous times. In contrast, in order to get an initial estimate of noise the equation would only have to be done once. This equation can be of good use in the early design stages because of the lack of information needed, as long as the assumptions inherent in this computation are understood.

$$SPL_{m\beta} = 40logM_e + 20logR/r + 20logh/c + 20logB + \Delta SPL_T + \Delta SPL_K - .9 \quad (1.1)$$

1.2.4.1.2 HSI Noise Based on the work of Arndt and Borgman, high speed impulsive noise is shown as a compressibility induced drag [17]. This model only requires the rotor blade chord length, effective rotor radius, and rotor radius for geometry inputs. The effective blade tip Mach number is the only dynamic input and the drag divergence Mach number is the only aerodynamic input required. There is a limit for the range of effective blade tip Mach number for this particular model [16].

Noise levels at each given harmonic frequency are given by Equation 1.2, where repetition would be required to get noise levels amount an entire frequency spectrum. This model works well as long as the limitations of flight conditions are maintained. If the design exceeds this, more extensive model may be required.

$$SPL_{m\beta} = 20log\frac{R_e}{r} + 20log[(M_e - M_{dd})c/R] + \Delta SPL_c - 21.6 \quad (1.2)$$

1.2.4.1.3 Loading Noise An example of a semi empirical model of loading noise is given in Equation 1.3 and based off of Lowson and Ollerhead [18] which does not include BVI noise or thickness noise. This methodology assumes an arbitrary point loading with random phasing and a thrust to drag to radial force of 10:1:1. The force ratios in actual

flight would vary. This would create uncertainty within the model since it relies on the assumption. The benefits of this semi empirical model is that the only geometry required is the number of blades, effective rotor radius, and the rotor azimuth angle. The flight conditions required by the model is the forward velocity, blade tip Mach number, rotor speed, and the total rotor thrust. No aerodynamic data is required for this particular model [16].

This model can be used to calculate noise of a tail rotor, but does not translate to other kinds of configurations. Adjusting for a tail rotor a different set of incremental sound pressure levels (δSPL_{tr}) would need to be used, based on hover or in flight conditions. Equation 1.3 provides an opportunity to capture loading noise without a full computational analysis of the aerodynamics of the system. While there are limitations in conditions, and assumptions of the forces, this model is useful in certain situations.

$$SPL_{m\beta} = 20log\frac{R_e}{r} + 20log\frac{T}{\rho c_o^2 R^2} + \Delta SPL_{mr} \tag{1.3}$$

1.2.4.1.4 BVI Noise BVI noise can be modeled using the work of Wright [19]. Since BVI is dominant in ascent and descent, this model only works from certain helicopter flight conditions. See Figure 1.6. The lift ratio...varies from about .15 for a conventional blade to about .07 for a blade with blade tip air injection.

Outside of this regime, BVI may not be present or another method would have to be used to capture any noise representative of BVI noise. This particular model is is more dependent on design parameters that pertain to the rotor specifically such as number of blade and the lift ratio ($\delta L/L_0$). The lift ratio pertains to differences between a conventional blade (constant chord, linear twist, square tip) or if blade tip air injection is used. With the limitations this model has due to flight conditions information such as total thrust, rotor speed, and air density are also required. Due to the many limitation this model has, it can

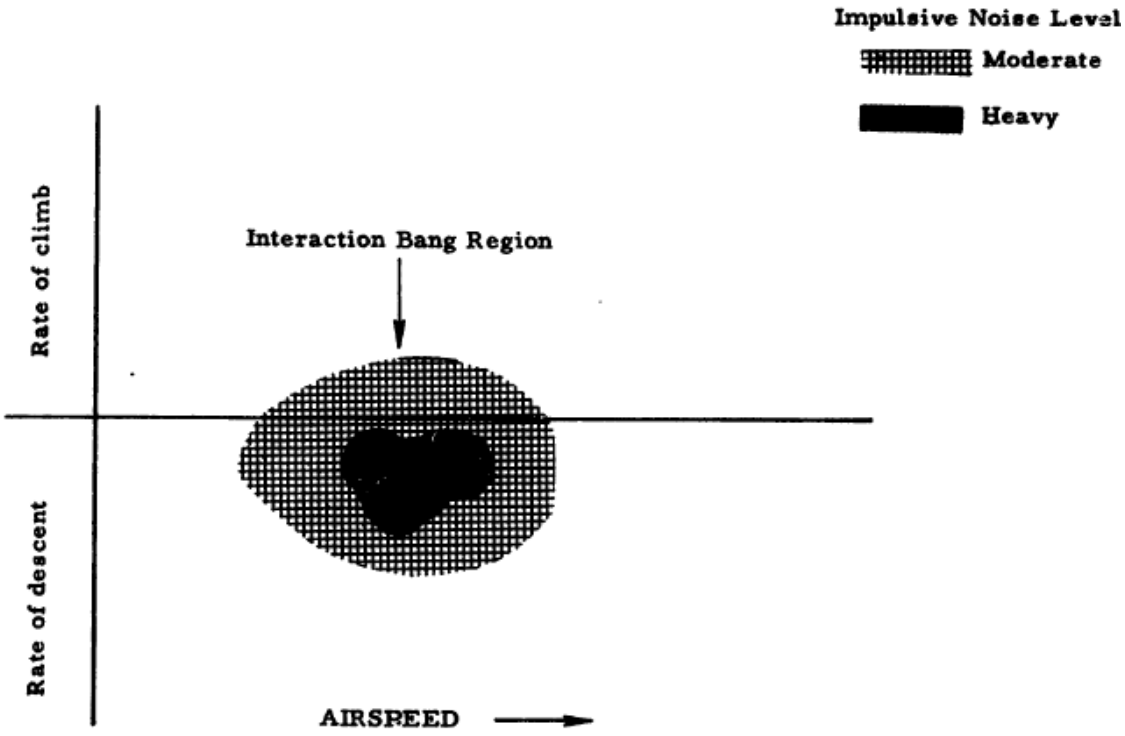

Figure 1.6: Flight region where this BVI noise model may be used[16]

only be used in very specific circumstances.

$$SPL_{m\beta} = 20log(\frac{\delta L}{L_0}cos\beta) + 20log\frac{T \cdot N}{\rho c_o^3 r} + \Delta SPL_{bv} + 190.2$$

(1.4)

1.2.4.1.5 Broadband Noise Since broadband noise is composed of many different sources, it is difficult to isolate each source and it is timelier to combine the sources since a similar output is given in each case. The model does not account for boundary layer, turbulent inflow and vortex interaction effects. In the model, the shape of the blade is unnecessary and only the total blade area of the rotor is required from the geometry. Dynamics require the thrust and rotor tip speed, while the only aerodynamic data needed is the average blade lift coefficient.

The model given in Equation 1.5 outputs sound pressure level [16] at the peak one-third octave band. The peak broadband noise can be calculated using another equation based on total thrust and rotor tip speed. This equations can be extended to other one third octave bands, but cannot be used for a full frequency spectrum analysis. More comprehensive computation would be required to achieve a full spectrum analysis.

$$SPL_{1/3} = 20log(\frac{V_T}{c_o})^3 + 10log\frac{A_b}{r^2}(cos^2\theta_1 + .1) + S_{1/3} + f(\bar{C_L}) + 130 \qquad (1.5)$$

$\bar{C_L}$ is the lift coefficient function and for most helicopters with a $\bar{C_L} \leq .48$ is $10log(\bar{C_L}/.4)$. This changes for helicopters with higher coefficients of lift. Since the vehicles under investigation for urban air mobility are not traditionally helicopter by design, the maybe be different or unknown. This model may not accurately reflect the noise signature of different

vehicles. For this noise source for urban air mobility systems, a different model or more extensive modeling may be necessary.

1.2.4 Analytical

Analytical models are based purely off theory and provide a closed form solution. This gives a response for a singular point and would be used similarly to a semi-empirical function. These models only work for one configuration because the theory would be based on a singular set up. Few inputs are required for these models. Some form of integration is common among this methodology. These models are very derivation focused and include multiple equations, which the final equation will be listed. Example rotor models will be given and advantages, disadvantages, and assumptions will be explained.

1.2.4.2.1 Thickness Noise Farassats thickness rotor noise analytical model will be discussed below. The model is particularly for rotors at high tip Mach numbers, but this paper was before the term high speed impulse noise was coined. The input parameters for this model are rotor motion, planform, and airfoil thickness distribution which is an advantage for design within the conceptual design stage. Unfortunately, this model is limited to hover and forward flight along with only a traditional helicopter configuration [20].

$$p(\overset{x}{\rightarrow}, t) = \frac{\rho_o c}{2\pi} \frac{\partial}{\partial t} \sum_{blades} \int \frac{d\tau}{r} \int_{meansurface} \frac{F'(\eta_1)(\eta_2\Omega - v_1)}{\sqrt{1 + F'^2(\eta_1)} sin\theta} d\Gamma \tag{1.6}$$

1.2.4.2.2 Loading Noise Filotas will be exampled for intensive loading and BVI noise, which at the time of the paper was referred to as blade slap. This model uses Lowson and Ollerhead [18] research similar to Peggs [16] work, where a Fourier analysis of a finite aspect ratio wing flying at uniform speed over infinitely long line vortices is used. The model fails to account for rotation which introduces a linear spanwise velocity gradient to the free stream. The magnitude of this velocity gradient unknown, but must remain small

compared to the free stream velocity for this model to hold true, which remains unrealistic in application. This can be accounted for using results from other papers since this effect is not negligible. This paper also discusses the importance for higher order terms to be investigated as well [21].

$$p(\overrightarrow{r}, t) = \frac{sin\varphi}{4\pi c_o r} \frac{\partial F(t - r/c_o)}{\partial t} \tag{1.7}$$

1.2.4.2.3 Broadband Noise In this noise type, an analytical model for a coaxial rotor configuration will be exemplified. This has been done by Blandeau, where he uses strip theory to treat the spanwise variations of aerodynamic quantities and blade geometries. Turbulent wake is assumed homogeneous and isotropic turbulence that is modulated by a train of wake profiles. The unsteady blade response is represented by unloaded flat plates, which removes the effect of angle of attack, which can be significant in non-isotropic turbulence. The tonal components are ignored in the model by assuming it is dissipated by the far field. This assumption is not necessarily accurate in application, but it is a common practice within the field [22].

$$p(x_0, t) = -\int_{s_2} \nabla \cdot [\frac{dF(x_2, \tau)}{4\pi r}]_t dS_2(x_2) \tag{1.8}$$

1.2.4 Numerical

Numerical models are based off of physics over time and are best used in a detailed design stage for more accurate data. Various inputs can be used within this modeling type. Generally speaking, the more information provided, the more accurate the noise data will be.

The more complicated the noise type, the more information that is required to have greater validity. For example, acoustic solvers can solve for thickness noise with just the geometry of the blade, while HSI noise needs more information such as CFD, in order to

predict compressibility effects and their location. All of the inputs are given to an acoustic solver which then propagates the source to the desired location, which can be a single observer point or a grid of observers. Figure 1.7 shows a generalized process for numerical modeling.

When it comes to acoustic calculations, the highest fidelity data is predicted when Computational Fluid Dynamics (CFD) data is given as an input [23]. While many commercial CFD packages have an acoustics module within them, they still use a form of acoustic solver. While the acoustic solver equation may be the same, the process may still differ in regards to time and acceptance in the aerospace community. When CFD data is unavailable, detailed flight control and dynamic data can be given as an input. Both of these calculations make numerical models rather timely [24].

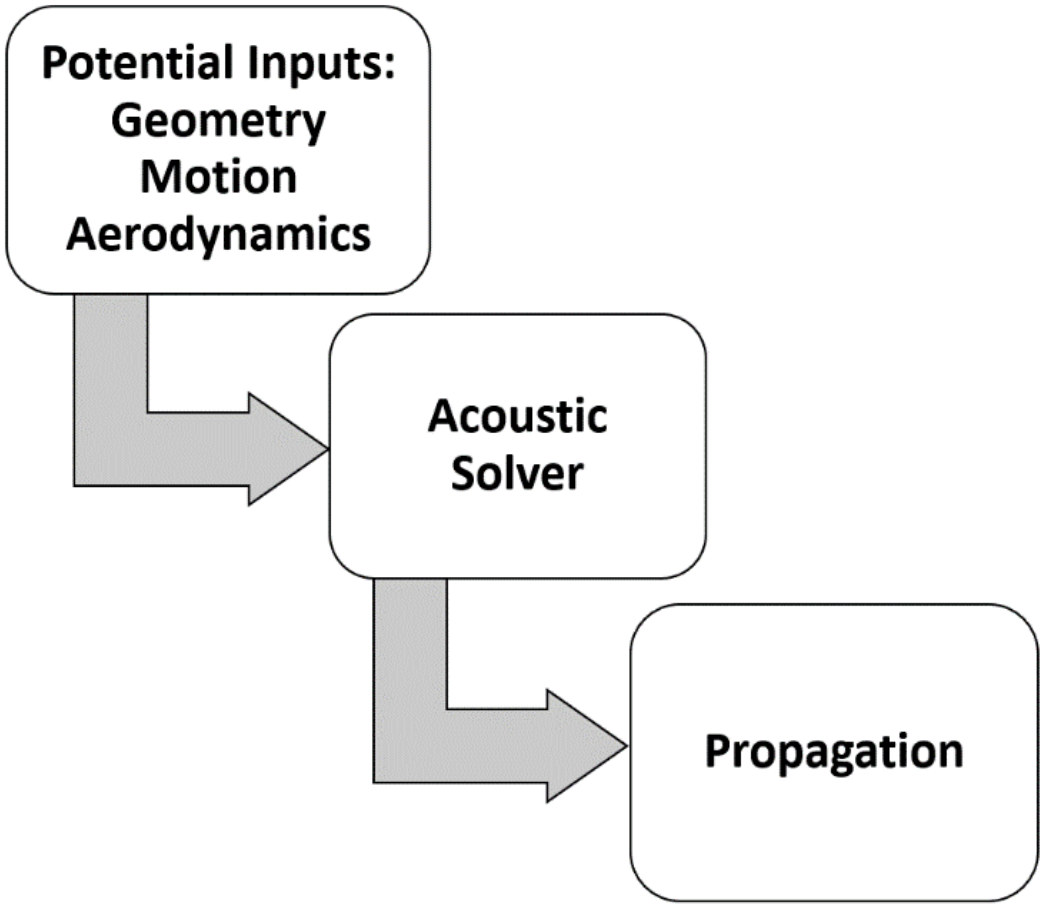

Figure 1.7: A flowchart that shows how numerical models would be used generically

1.2.4.3.1 Kirchoff Formulation The Kirchoff Formulation for moving surfaces uses physical sources represented by mathematical sources on the surfaces. The governing equation is an inhomogeneous wave equation where all the physical sources are on a fictitious surface. In this methodology there is no volume integration necessary, which makes it computationally less expensive. Until about 20 years ago, Kirchoff could not be used for aeroacoustic significance because CFD was underdeveloped. It is less popular because the source terms are not as easily traceable and/or isolated which makes it less ideal for

designing [25, 26].

$$\begin{aligned}\Box^2 p'(x,t) = &-(\frac{\partial p'}{\partial t}\frac{M_n}{c} + \frac{\partial p'}{\partial n})\partial(f) \\ &- \frac{\partial}{\partial t}(p'\frac{M_n}{c}\partial(f)) \\ &- \frac{\partial}{x_i}(p'\hat{n}_i\partial(f))\end{aligned} \tag{1.9}$$

Where $M_n = v_n/c, p'$ is acoustic pressure, t is time, and c is speed of sound.

1.2.4.3.2 Ffowcs Williams Hawkings Equation One of the most commonly used acoustic rotorcraft numerical models is PSU-WOPWOP which is a code developed by NASA and utilizes Ffwocs Williams Hawkings (FWH) acoustic solver [24]. This is an extension of Lighthills acoustic analogy with surfaces using surface and volume integrals. It uses Navier Stokes equations along with an inhomogeneous wave equation. Typically, the quadrupole term is excluded in this methodology to save time, but can be included if desired at computational expense. The quadrupole is primarily important in transonic or supersonic cases. The FWH is a popular acoustic solver due to its ability to isolate sound sources which can be used in design stages to properly diagnose the noisiest source [25].

Equation 1.10 is the FWH equation and is typically solved through Farassat's equation which excludes the quadrupole term. This can be included in cases where supersonic noise is desired to be captured.

$$\begin{aligned}\Box^2 p'(x,t) = &\frac{\bar{\partial}^2}{\partial x_i \partial x_j}[T_{ij}H(f)] \\ &- \frac{\partial}{\partial x_i}[(P_{ij}\hat{n}_j + \rho u_i(u_n - v_n))\delta(f)] \\ &+ \frac{\partial}{\partial t}[(\rho_o v_n + \rho(u_n - v_n))\delta(f)]\end{aligned} \tag{1.10}$$

Where T_{ij} is the Lighthill stress tensor, u_n is the fluid velocity in the direction normal

to the surface $f = 0$ and v_n is the surface velocity in the direction normal to the surface.

1.2.5 Literature Summary and Gap

Each model comes with its limitations as well as its best use cases. The level of fidelity of a model is proportional to what stage the design is in. In some situations, where less information is known about the design and flight configuration, such as the conceptual design stage, a semi-empirical model can be more useful. While, the more information known about the final design, the more accurate the acoustic signature can be predicted using a numerical model. The desired fidelity for this study is in the semi-empirical modeling stage where not very much is known about the design, and the acoustic signature is a rough estimate. This way the design can be easily changed early on in the design process to avoid complications later on.

All of the acoustic models discussed above is based around the wave equation within different applications. While the semi-empirical models are extrapolations of testing data to bypass theoretical applications, the theory is still present in the real life physics. This thesis provides a methodology for creating a semi-empirical model without the troubles of testing. Which would provide a simplistic model to be used in an earlier design stage.

As seen above by the aforementioned models, the level of fidelity of a model is also proportional to how flexible the model is when it comes to various designs. The semi-empirical models only are valid for a traditional helicopter configuration, while numerical models like WOPWOP can work for any configuration of rotorcraft. The literature gap lies here, as identified by the likes of Brentner and NASA [4, 27], where there is not semi-empirical models for various rotorcraft configurations. With new research areas such as Urban Air Mobility on the rise, it is important to have lower fidelity models such as semi-empirical models for various rotorcraft configurations for the conceptual design stage. This thesis provides an approach for filling this literature gap.

CHAPTER 2

PROBLEM FORMULATION

If urban air mobility vehicles were modeled today, any of the aforementioned modeling could be used with various advantages and disadvantages. It is dependent on the particular vehicle and mission profile to be able to assess these pros and cons. The results can change dramatically based on the situation, therefore, the problem formulation is critical in analyzing what is the solution.

In an ideal world, these vehicles would simply just be built and flown with flight test measurements or put into a wind tunnel with microphones. This would be the most accurate, highest fidelity approach. This would allow for testing of many different flight conditions and design parameters and empirical relationships to be formulated from those variations.This option tends to be extremely costly and timely. It is also desired that noise is estimated before the production, in the conceptual design stage.

Calculating the surface pressures on the system in question is as accurate as the CFD performed. Therefore, the level of fidelity of CFD is just as accurate as the level of fidelity for acoustic modeling. The acoustic solver would convert the surface pressures to acoustic pressure and propagate the data to the desired receiver.

The highest fidelity that modeling can provide is using CFD along with Computational AeroAcoustics (CAA). This method can be extremely timely and very, computationally expensive because it provides the most accurate process. CAA is one of the highest fidelity propagation methods. This would require a lot of knowledge about the final design[28].

One of the lower fidelity approaches to conceptual noise design of UAM vehicles would be to use the semi-empirical models for rotorcraft with some correction factors applied for different designs and flight conditions. The correction factors would be calculated by using some CFD data points of different configurations in order to better represent the designs.

Another lower fidelity approach would be to derive an analytical model directly from theory. Unfortunately, this would only work for one given situation because the derivation would only be for one situation at a time. In many analytical models such as ones discussed above, they only consider tonal or broadband noise at a time. The derivation would have to be repeated for various configurations, flight conditions, and noise types.

With UAM being under development, the market is still considering many different concepts for these vehicles. Designers may not know all the particular design or configuration parameters for them, therefore using a model with few inputs and fast computation would be ideal. Since there are limited semi-empirical models for these non-traditional configurations and the expense of production and testing for real world concepts, opportunities for trade offs and design exploration become apparent. To avoid testing, a higher fidelity model would be used instead, and in order to avoid finalizing design details too soon a lower fidelity model would be created for the entirety of the conceptual design stage.

Since both, the configuration and the more detailed rotor design may be unknown at this design stage, this research aims to relate design and configuration parameters to the output of noise. This becomes the overarching question for this research because the exploration is around configuration and the desire is to quantify the noise outputs. If design and configuration parameters can be related to noise outputs, a model can be built to replicate it. The desire is to create a model that can fill a literature gap within the conceptual design stage. It is known that parameters affect noise, but by how much and in what way? Which brings us to the following hypothesis.

Hypothesis I: If design and configuration parameters can be related to noise outputs by controlled detailed modeling, a simplified model can be built to replicate it.

This hypothesis will be tested by controlling the design inputs of a rotor system and investigating the noise outputs to see if a relationship exists. The purpose of this experiment will be to see if the outputs of the system can be controlled by the inputs. After

the inputs and outputs of the system are analyzed, trends can be looked at across all three configurations, and an attempt at a representative model can be done.

It is not known whether trends can be identified and whether they would be a well enough fit to be a usable model. An acceptable model will be determined by the fit of the model to the data results through a low standard deviation, few to no outliers, and an R squared value close to one. This concept gives the final hypothesis.

Hypothesis II: If noise trends are apparent across various configurations, then acoustic considerations can be accounted for in the conceptual stage across the UAM design space of interest.

This hypothesis is going to be tested by the development of a low fidelity acoustic model to look at the inputs and outputs of design and noise on a larger long term scale. By proving that computational time can be reduced, while still showing a certain level of fidelity in results, the hypothesis can be proven correct. The level of fidelity will be determined by the R squared value of the model fit, and if the data looks visually consistent.

If this hypothesis is proven to be correct, this would be a significant contribution to the field, allowing designers to design with noise concerns early in the design process. This would help to mediate noise in UAM vehicles before they even start to integrate into society. This would make them more accepted by society.

The following research questions center around the approach and model development, which are more open ended.

As the design space for complex rotorcraft concepts increases, modeling tools in the conceptual design stage are more desired. Designers need to be able to tell early on in the design process whether a configuration will have acceptable noise levels. There is no historical data on these vehicles because of the recent development of this field and the

amount of time it would take to experimentally test each of these concepts to develop a representative equation would not only be timely, but expensive. This thesis aims to develop an approach to creating a model to help aid in design within the conceptual design stage. The approach calculates the noise of various configurations using a higher fidelity numerical model to create a fast lower fidelity model with minimum inputs. This leads to the following overarching research questions.

Research Question: How is the configuration space for rotor noise analysis quantified?

Research Question: What are the most important parameters to consider when designing according to rotor noise?

The important design characteristics have been looked at by previous work, but not yet quantified. These previous studies identify the parameters of interest for this study. The following tables below list the parameter of interest, including design and configuration parameters, and the limits to which they varied. These parameters and their limits were taken from literature. These design parameters were chosen because they are commonly found to be influential of the acoustic signature of rotors from previous models. The ranges and designs were chosen to be representative of rotors that designers are looking into for UAM vehicles. This means that these parameters need to be practical and that the range needs to be big enough to capture the trends in acoustic signature, but small enough that the study does not become overly computationally taxing. One of the goals for this study is to negate negligible parameters and quantify the influential parameters.

Starting with the configuration parameters, vertical separation was chosen as an important parameter based off the the work by Schatzman [1] and the limits were chosen based off a combination of her work as well as other UAM company interests and designs. Duct length and width were chosen as parameters based of the work by Zentichko [13] and the limits were chosen based off a combination of his work as well as other UAM company

interests and designs.

The design parameters were chosen through common parameters that are influential to the acoustic signature within the work of Pegg [16] along with Ahuja [5]. The corresponding limits were chosen in hopes to encompass the effect on the acoustic signature, but small enough to fit the scope of this project. Companies that are currently designing or interested in designing UAM vehicles were considered [29, 30]. See Tables 2.1 through Tables 2.3.

It is important to note that the following run matrices do not attempt to answer research question 2 directly. Research question 2 will be answered based on the outcome of this research. The results should show whether or not the chosen ranges are large enough to encompass the trends that influence the acoustic signature.

Table 2.1: Run matrix for the ducted rotor configuration

Configuration: Ducted		Min	Max
Configuration	Duct Width (Airfoil Thickness)	10%	15%
	Duct Length (Chord)	10	15
Design Parameters	Rotor Radius(ft)	3	15
	Blade Tip Mach Number	.45	.65
	Number of Blades	2	5
	Chord (ft)	.25	1
	Airfoil Thickness (Thickness to Chord)	10%	15%
	Blade Twist	5	10
	Taper Ratio (Linear Distribution)	40%	100%

Table 2.2: Run matrix for the coaxial rotor configuration

Configuration: Coaxial		Min	Max
Configuration	Vertical Separation (Separation/Rotor Diameter)	.25	0.5
Design Parameters	Rotor Radius(ft)	3	15
	Blade Tip Mach Number	.45	.65
	Number of Blades	2	5
	Chord (ft)	.25	1
	Airfoil Thickness (Thickness to Chord)	10%	15%
	Blade Twist	5	10
	Taper Ratio (Linear Distribution)	40%	100%

Table 2.3: Run matrix for the *both* (ducted coaxial) rotor configuration

Configuration: Ducted Coaxial		Min	Max
Configuration	Duct Width (Airfoil Thickness)	10%	15%
	Duct Length (Chord)	10	15
	Vertical Separation	.25	0.5
Design Parameters	Rotor Radius(ft)	3	15
	Blade Tip Mach Number	.45	.65
	Number of Blades	2	5
	Chord (ft)	.25	1
	Airfoil Thickness (Thickness to Chord)	10%	15%
	Blade Twist	5	10
	Taper Ratio (Linear Distribution)	40%	100%

These design parameters were chosen because they are commonly found to be influential of the acoustic signature of rotors from previous models. The ranges and designs were chosen to be representative of rotors that designers are looking into for UAM vehicles [29, 3]. This means that these parameters need to be practical and that the range needs to be big enough to capture the trends in acoustic signature, but small enough that the study does not become overly computationally taxing. It is important to note that the ranges for the parameters will be directly linked to the outputs. These were reasonable ranges chosen

for design variation for this study. Certain parameters are more important for UAM design considerations and therefore may have larger ranges. The objective of this thesis is to develop an environment in which this analysis can be done easily as parameters and ranges change.

Along with important design parameters, it is important to distinguish important flight condition parameters as well. It is desired that design parameters are decoupled from flight condition parameters, in order to develop a function of only design parameter inputs. Unsteady effects in various flight conditions lead to studying different noise types in hover first[31]. Hover does this most efficiently due to reduced flight condition effects on the acoustic signature, since there is no tendency towards any one noise type. This also allows for reduced computational expenses as well as better reflects UAM vehicles since hover is often demanded of them. The potential drawback to looking at hover, is that hover would be used mid-flight, therefore the highest altitude, meaning the noise source is the farthest away from humans. It may be more of interest in the future to look at landing and take off flight conditions as they would place the noise most nearest to people to disturb. For this experiment, it is necessary to keep the flight condition consistent as not to add too many variables.

Research Question: How would the effect of parameters on different noise types be predicted?

This question addresses how to about the process, which is by running several numerical studies to identify trends to build a semi-empirical relationship. First the configuration is defined, and then cases are run to identify the influential parameters and their sensitivities. Then the correction function would be built to fill the literature gap. Figure 2.1 shows a flow chart of how this research will be addressed step by step.

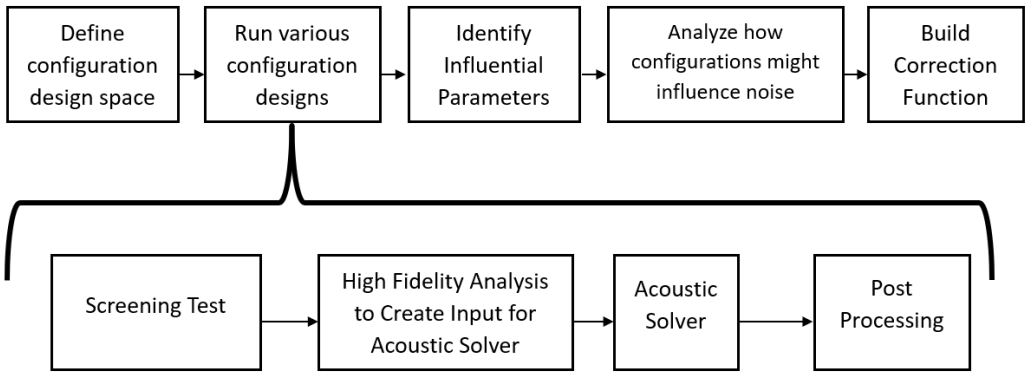

Figure 2.1: Overall flowchart for this thesis

Research Question: How would the interaction of architectural configurations and noise be predicted?

Rotorcraft configurations can influence various performance parameters as well as the acoustic signature of the vehicle. Since all of the parameters are so heavily connected, it is important to look at all the various ways parameters can be varied. This study looks at the variation of RPM, geometry of the vehicle, and configuration thrust.

RPM is heavily linked to frequency through BPF as previously mentioned. Frequency can easily affect the way people perceive how loud a noise can be. Looking at the equal loudness chart below (Figure 2.2), one can see how lower frequencies are heard as louder than higher frequencies at the same amplitude. It is important that RPM is matched throughout comparable configurations so the human response is similar.

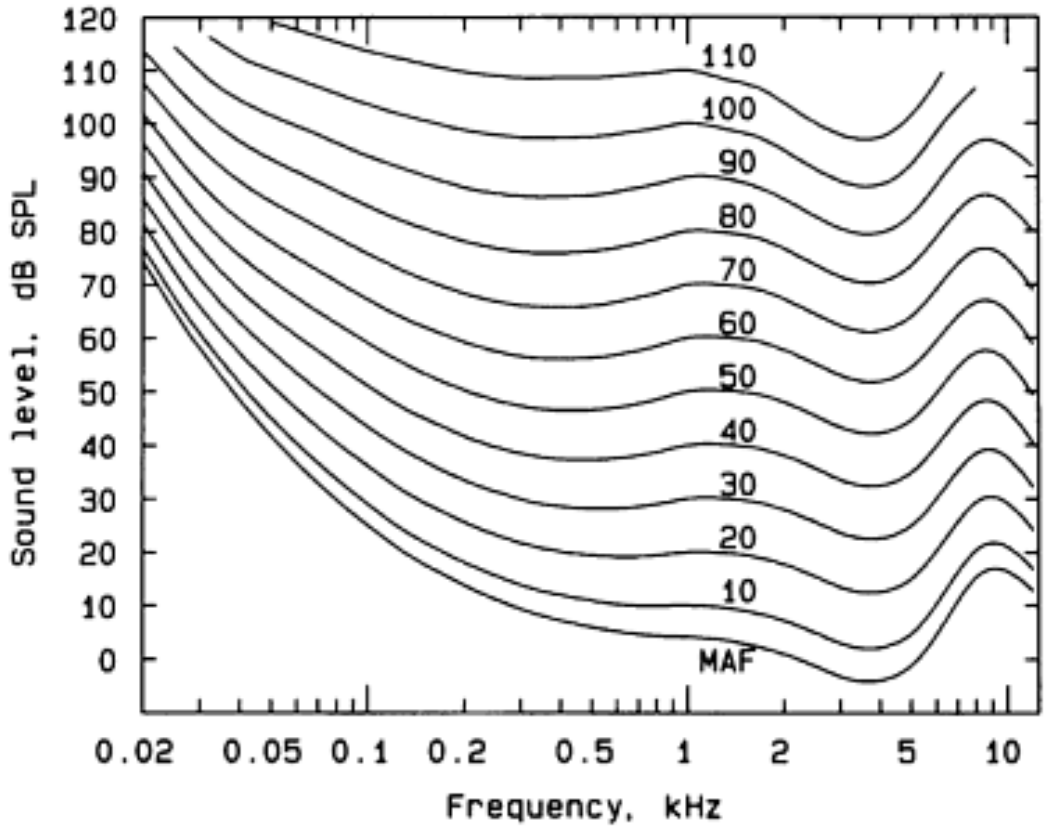

Figure 2.2: Equal loudness curves [32]

The geometry is what creates the design and can highly influence the acoustic signature. In order to properly and easily map the change in design parameters to the change in noise, the geometry between comparable configurations should be matched.

It is known that some configurations can provide the same thrust with smaller geometry, such as a ducted rotor can be smaller than an open rotor and still provide the same thrust. Since some of the configurations provide more thrust with the same geometry and RPM and geometry would be matched, there must be a mismatch of configuration thrust. This creates a design exploration within acoustics and rotorcraft design parameters, which is useful within such a new field of research. The drawback of this choice is that optimal performance will not be looked at and considered, all variations of performance will be considered, even though some would never be put into actuality. The intent of this work is

to create a model of few inputs that could give an estimate of noise of a particular vehicle. That being said, after the model is created a vehicle of optimal performance can be designed and inputted into the model to calculate the acoustic signature.

2.1 Designing the Experiment

This thesis aims to develop a process for developing a semi-empirical model, without needing physical testing data. The most accurate data, next to test data would be numerical modeling. The process seeks to prove that this is an effective and accurate way to develop a new lower fidelity model for the conceptual design stage.

It is desired to create a methodology in which non-traditional rotorcraft designs can be quantified and characterized in a parametric environment. The parameterization of this experiment is crucial due to the need to be discussing the vehicles in terms of design variables for ease of change and flexibility when adjusting designs.

Since noise is generated by a pressure difference, and object disrupting the air, the design is the primary focus and cause of noise. The parametric conceptualization of rotor designs is seen in previous research's semi-empirical models. Looking at current history of design and its effect on noise, allows for important parameters to be identified. This allows for the reproduction of run matrices or an expansion on them.

Afterwards a DOE should be selected in order to optimize time and computing expenses. It should be noted that the particular DOE chosen will influence the type of representative model in the outcome. For this situation a screening test DOE is used to provide results at a range of high, medium, and low input parameters.

The flight condition and aerodynamics are important to consider since they are very impactful to the acoustic signature of the vehicles. In this situation is the system flying in hover and the design will be the baseline for the experiment. The design will be simulated to be typical flying conditions, which for these vehicles means lower flying, subsonic conditions. From simulated flying conditions, surface pressures will be extracted and then

converted to force to know the force acting on all points of the rotor blades.

The design and resulting forces will be converted into acoustic pressure and decibels. This will be the final results of data which will then be analyzed for trends and representative model fits. Influential parameters will be identified using bootstrap forest partitioning, providing an order, as well a percent contribution to the importance. Several model regressions will be attempted to fit the data results. They will be quantified and compared through several graphs, such as actual data plotted by predicted data, as well parameters such as R square and standard deviation. The model fits along with the quantified acoustic parameters are the final objectives of this these which attempt to prove the hypothesises.

The hypothesises will proven by the trends within the results. If there is apparent trends between noise and the inputs, there is an amount of control over it. The success of these trends will be determined by particular variables that quantify how strong a trend is, and how well a mathematical model can fit the data. This ultimately, will show whether or not a representative model can replace a modeling within the conceptual design stage.

2.2 Noise Metrics

How the results would be compared is an important area of interest. Noise is measured in decibels, but various different metrics can be applied in order to better represent the situation under investigation. The Handbook of Aircraft Noise Metrics lists 21 different noise metrics, which are all calculated very differently [33]. Some metrics are over various periods of time, some are instantaneous, others can be skewed to give a higher noise rating for higher or lower frequencies. This can give widely different results based off what metric is being used. This can make it difficult to determine which noise metric would be optimal for the case study.

Many noise metrics take into account other factors that can influence human perception of noise. Psychoacoustics is a big field of study because in many situations it is easier to mitigate human perception of noise rather than the actual noise. Usually this refers to

controlling the most annoying part of the noise and in many situations noise can be mapped to annoyance [34]. This requires human subjects to measure responses, which is out of the scope of this project. In some metrics, some general pyschoacoustic considerations are encompassed within the metric. Day Night Level (DNL), is an example of a metric that has a higher penalty for noise at night due to the increased annoyance at that time of day [33]. These considerations are generalized and based off of current vehicles. The acoustic signature of a UAM vehicle has already proven to be very different than current vehicles [3, 4] and, therefore, these may not hold true.

Acoustic metrics can either be over a period of time or instantaneous [33]. It is unknown currently how long these vehicles might be in hover and, therefore, noise over time may skew results. It is also undecided currently at what time of day these vehicles may be flying. Some metrics take into account time of day into their calculations which is desired to be avoided. For this research, an instantaneous value is preferred to compare a maximum sound level rather than comparing noise over time [35].

UAM vehicles overall are still undergoing research in design in various configurations which each give a very different acoustic signature. Compared to traditional aircraft or rotorcraft, the acoustic signature of UAM vehicles is vastly different and the same noise certification cannot be used. The Federal Aviation Administration (FAA) has not given noise certification to UAM vehicles; therefore, an optimal noise metric has not been chosen [35].

This area is a research project in and of itself and while this area is still being developed, a metric still must be chosen for the current project in question.

Noise has many different aspects to it and it is common to discuss noise in multiple factors at once, such as loudness per frequency band. In order to identify possible trends in the data, the data must be able to be ranked in a single value. Overall Sound Pressure Level (OASPL) allows for a single value across any particular time frame, as well as across all frequency bands. OASPL in dB has been chosen as the noise metric for this project due to

the encompassing of frequency and volume into one number. Multiple other noise metrics can be outputted from acoustic solvers for comparison purposes, while OASPL will be used to determine the parametric sensitivity of noise.

2.3 Experimental Setup

Many codes could have been chosen for this study, but since this is still a new research field, it is important to chose codes that allow for some flexibility in use. This will provide ability continue the use of the as the field grows. The areas of the experiment can be divided into design, CFD, and acoustical analysis.

OpenVSP is an open source code written by NASA that allows for ease in building new rotorcraft specific geometry with the built in geometry design features. The geometry can be altered by predefined parametric design variables. This helps to visualize the designs being tested to ensure it is the desired design. It also has python API capability for ease of use.

Once there is a rotor system created, the flight environment and java script will be generated using StarCCM+. CFD is the necessary process in order to properly capture the flight conditions, the complexity of the configurations, and generating the surface pressures on the blades. This java script becomes the baseline script for the CFD analysis. The parameters from the run matrices can be identified and varied using a script which generates the full set of cases. StarCCM+ was chosen due to its capabilities of replicating the flight conditions desired while also being able to export in a format compatible with PSU-WOPWOP.

Once the CFD cases are fully executed, surface pressures from the blade can be exported and the resulting forces can be calculated. This allows for the geometry and loading to be inputted into PSU-WOPWOP. This particular acoustic solver allows for speed in calculation, while keeping in consideration of configuration and design aspects.

The output of PSU-WOPWOP gives the final form of the data, which is OASPL values

along with separated thickness and loading noise values. The OASPL values along with the varied inputs allow for a bootstrap forest partitioning to be done, in order to evaluate influential parameters. JMP allows for various kinds of statistical analysis. Multiple fits of models can be extracted onto the data. Looking at influential parameter trends, along with well fitting models, an optimal model to represent that data can be decided upon. This model of best fit can be used to substitute this entire process for a quick noise estimate of a design in the conceptual design stage process. A summary of this step by step process is in Figure 2.3.

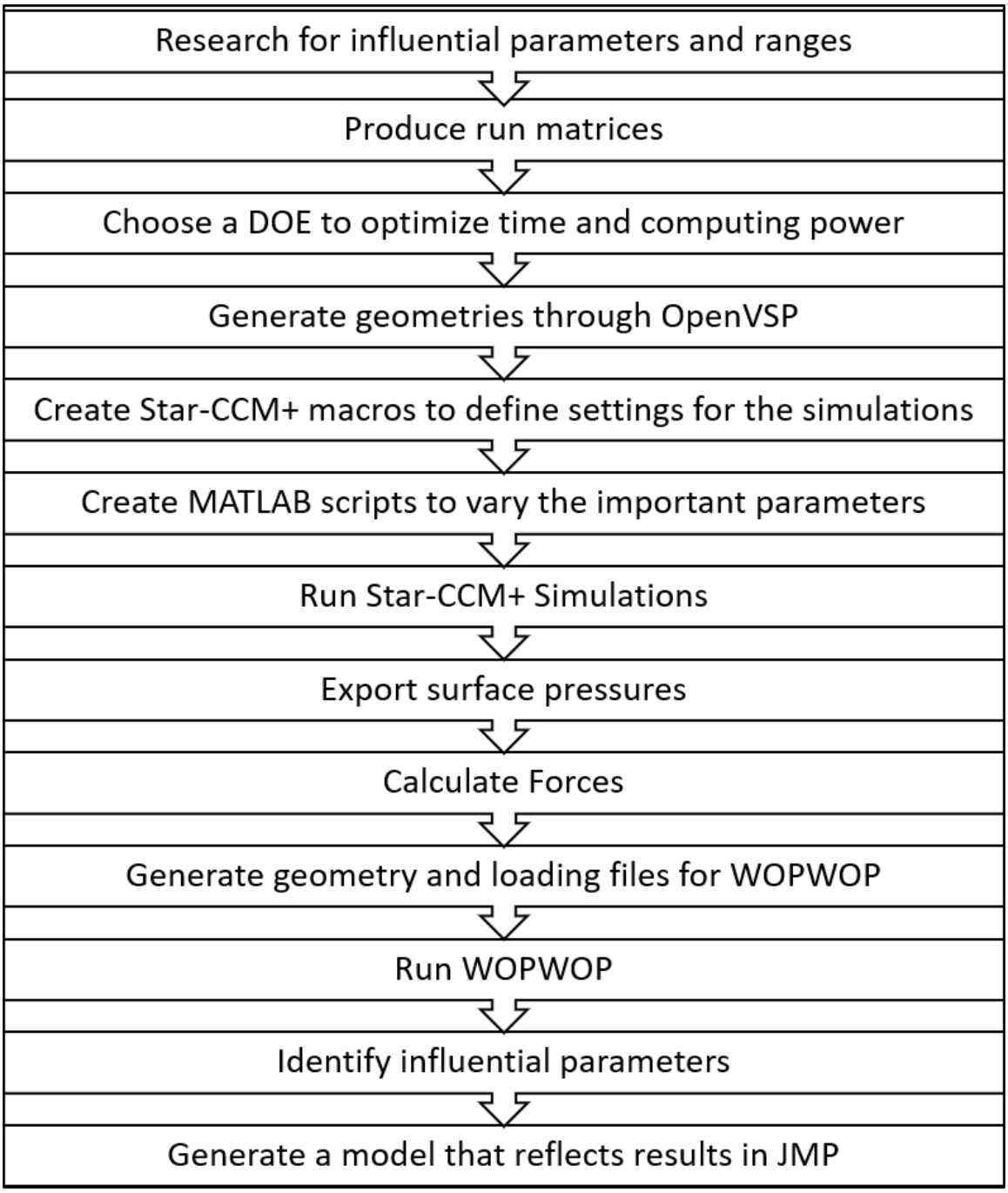

Figure 2.3: Step by step process

CHAPTER 3
PROPOSED TECHNICAL APPROACH

This section details how this project will be executed including the format the results will be in, as well as the limits of the design space. The overarching goal of this research is to develop an approach to model acoustics within the conceptual design stage. Therefore, certain aspects of accuracy are outside the scope of this project. Results may include a certain amount of error. If error were to be reduced, trends would still be found through this methodology.

3.1 Defining the Configuration Space

The configuration space that is defined hopes to encompass the change in acoustic signature that the design parameters may have. Design parameters were chosen based on past research on what are large drivers of noise. The respective ranges were chosen to fully encapsulate the change in noise without being too computationally taxing. The configurations being looked at, as previously discussed, are a ducted rotor, coaxial rotor, and a ducted coaxial (*both*) rotor. For each parameter, minimum and maximum range values were identified based on reviewed literature.

3.2 Running Various Configuration Designs

This section details how the cases that are chosen would be run and processed.

3.2.1 Screening Test

With the many parameters of interest, along with the wide range for these, a rather large design space has been discussed. This can lead to numerous runs and be extremely compu-

tationally expensive.

Designs of Experiments (DOEs) are typically used to minimize efforts, while maximizing information [36]. This particular research is interested in understanding the system, especially in extreme cases. A DOE that considers the maximum and minimum values changes would be of most usefulness.

A screening test looks at the spread of the data, between a high, middle and low value of the specified ranges. This DOE efficiently estimates main and quadratic effects for often fewer trials than traditional designs. In order to reduce the number of runs within this research, a screening test has been chosen as a DOE [37].

Continuous factors will be considered within this DOE instead of categorical factors because the design parameters can vary inside the range. This DOE allows the sensitivity of the inputs to be analyzed and quantified. Negligible inputs can be negated, and influential parameters can be ranked [37].

3.2.2 Input into Acoustic Solver

Since numerical models can have several inputs it is important to note the level of fidelity that is required for this study. The final representative model would be of low fidelity in order to satisfy the low computational time needs. Collins discusses both a low fidelity and a higher fidelity process for the creation of scaling functions to map low fidelity results to a high fidelity domain [23].The configurations that are being analyzed are more advanced and require higher fidelity to understand the effects that are happening.

It has already been noted that numerical models can take into account geometry, motion and airloads, as well as CFD. The final representative model would be a function whose inputs are the parameters that have been previously mentioned. For the study, parameter dimension limits have been specified previously. Motion and air loads would be required for this study, but limited information in this area is needed for the representative model. CFD is the highest fidelity and is the most appropriate for this study, while other inputs can

be used if CFD is too high in computational time [24, 25]. A lower fidelity study may be done, only using geometry and motion, without CFD, as shown by Collins previous study [23]. While this remains a potential option, it may produce less accurate results to some degree.

3.2.3 Acoustic Solver

An acoustic solver would input the surface pressures from CFD from the geometry as an impermeable surface. This means that they are on the body of the geometry surface and that they do not admit a normal velocity component. This form of acoustic surface is best used when advancing tip Mach number is lower than 0.85 and there are no nonlinear effects. For hover, it is recommended that pressure and geometry is stored in time intervals of two to five degrees as the blade rotates [24]. Motion and airload data would be specified in a separate file. The acoustic solver would propagate the noise using atmospheric absorption and a standard atmosphere table to the observer distances. The observers (receivers) within the acoustic solver will be placed in the far field from the source. A grid of observers will be used due to the directionality of rotorcraft. Many different noise metrics can be outputted and analyzed, but the primary output used for the system analysis and representative equation will be in OASPL (dB).

3.2.4 Post Processing

Since the results will already be in the appropriate noise metric, the post processing will primarily be done using statistical analysis software. In this step, the noise output will be related and correlated to the various input parameters. The influential parameters will be calculated for their ability to predict an outcome using bootstrap forest partitioning to evaluate the contribution of predictors on the response [38].

3.3 Identifying Influential Parameters

The conceptual design stage does not require a high fidelity analysis. Therefore, only the significant parameters are necessary to include in this study. Not every variable will be a significant driver of noise and some may be negated [36].

Typically the top eighty percent of the total influential parameters are considered significant. Sometimes a cross term is listed as significant, which means one or both terms are significant. Parameters below this eighty percent will be considered negligible [36]. It is important to note there may be parameters that are significant, but have not been included in this study due to the scope of the project.

3.4 Analyzing Trends

After identifying influential parameters, the negligible parameters will be ruled out. This allows investigation into the significant influencers of noise. Parameters may increase or decrease the noise in particular areas. For example, Blandeau discusses the inversely proportional change in tonal and broadband noise regarding the change in vertical separation [22]. The overall effect of increases or decreases in total noise will be looked at. The percent contribution of each significant parameter will be considered in order to quantify the amount of influence.

3.5 Representative Model

Once negligible parameters are ruled out, and trends are analyzed of significant parameters, a potential representative model will be generated based on how the results look. There are many different types of models that may fit the data appropriately [39]. This cannot necessarily be predicted at this point because it is unknown what particular trends may lay in the results.

CHAPTER 4
INPUT INTO ACOUSTIC SOLVER

4.1 Geometry

The geometry was generated using OpenVSP and the parameters that have been discussed previously. This was generated using a python API that connects with OpenVSP [40]. Python allows the generation of the geometry to be automated parametrically.

OpenVSP has many baseline vehicles or aspects of vehicles that can be highly altered. This project utilized the baseline propeller, duct, and disc geometry and adjusted the model until all features corresponded with the run matrices. A python script was written that takes the parameters from the run matrices and the DOE and varies them accordingly to build a full set of geometries for each case. Geometries were imported to Star CCM+ as an .igs file in order to separate components of the geometry within CFD, such as rotating parts and non-rotating parts.Figures 4.1 through 4.3 show example geometries of each of the configurations.

These rotors are assumed to be rigid for simplification purposes. For the coaxial cases and the *both* cases, the rotors are not connected. In actual application these rotors would be placed on the same shaft. This geometry was assumed for modeling purposes. The center body is modeled as a disc that connects the rotors. The center body is adjusted for the worst case scenario (largest twist, thickness, and chord sizes), and then scaled for the other cases. In some cases, it should be noted that the center bodies are rather large and unrealistic. This may effect noise, but since it was scaled appropriately, the trend should be the same across all cases.

Tip clearance has been shown to be a notable parameter when it comes to noise and design [41]. In order to keep the number of parameters of interest low, tip clearance was not

included; it should be noted that for all ducted geometries, a tip clearance of approximately 0.5% of the rotor radius was used.

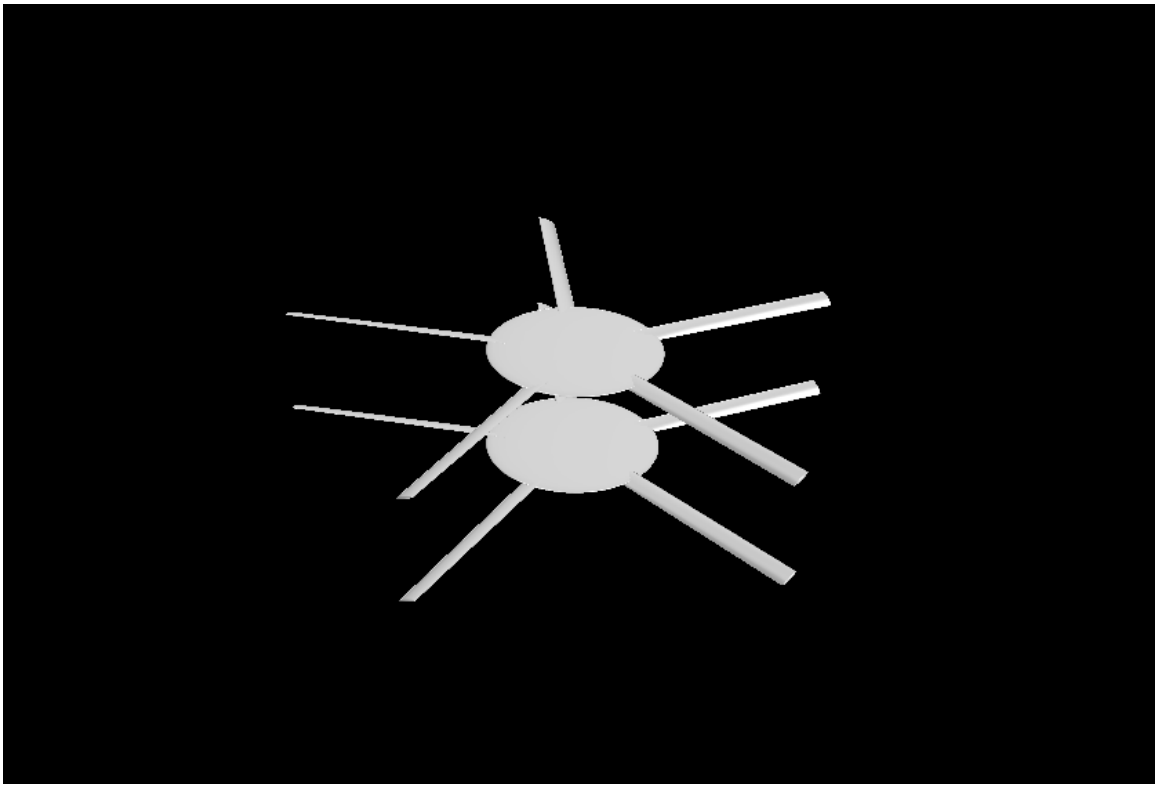

Figure 4.1: Coaxial case 1 geometry

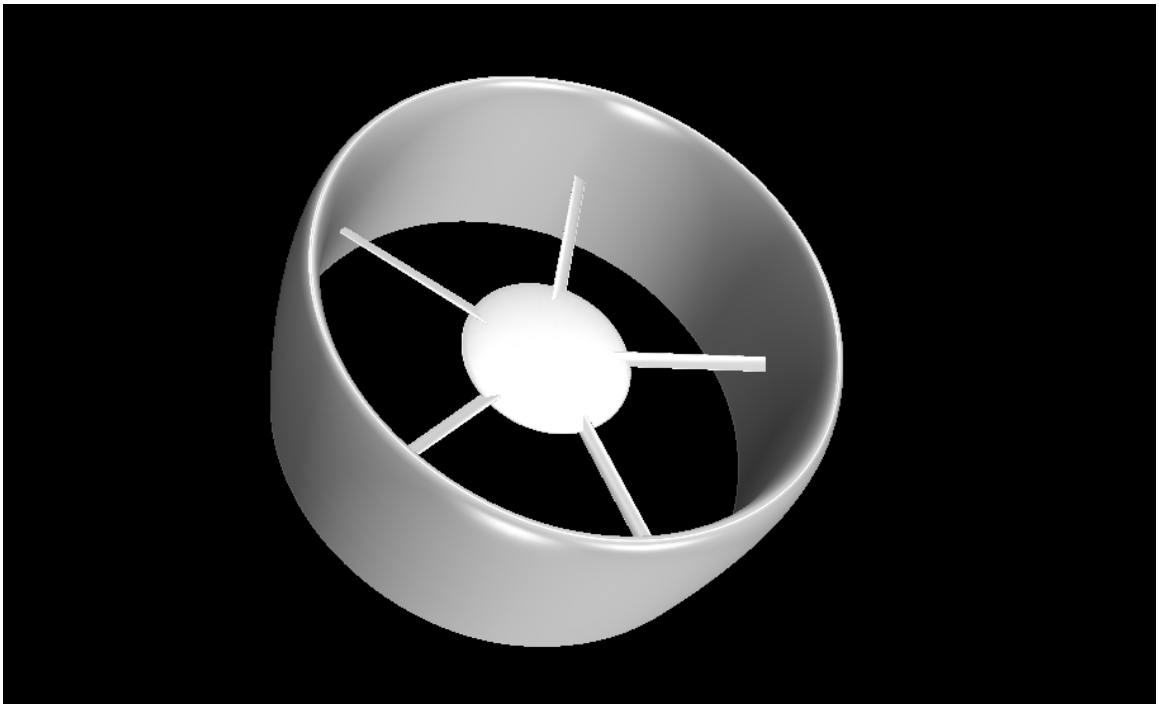

Figure 4.2: Ducted case 1 geometry

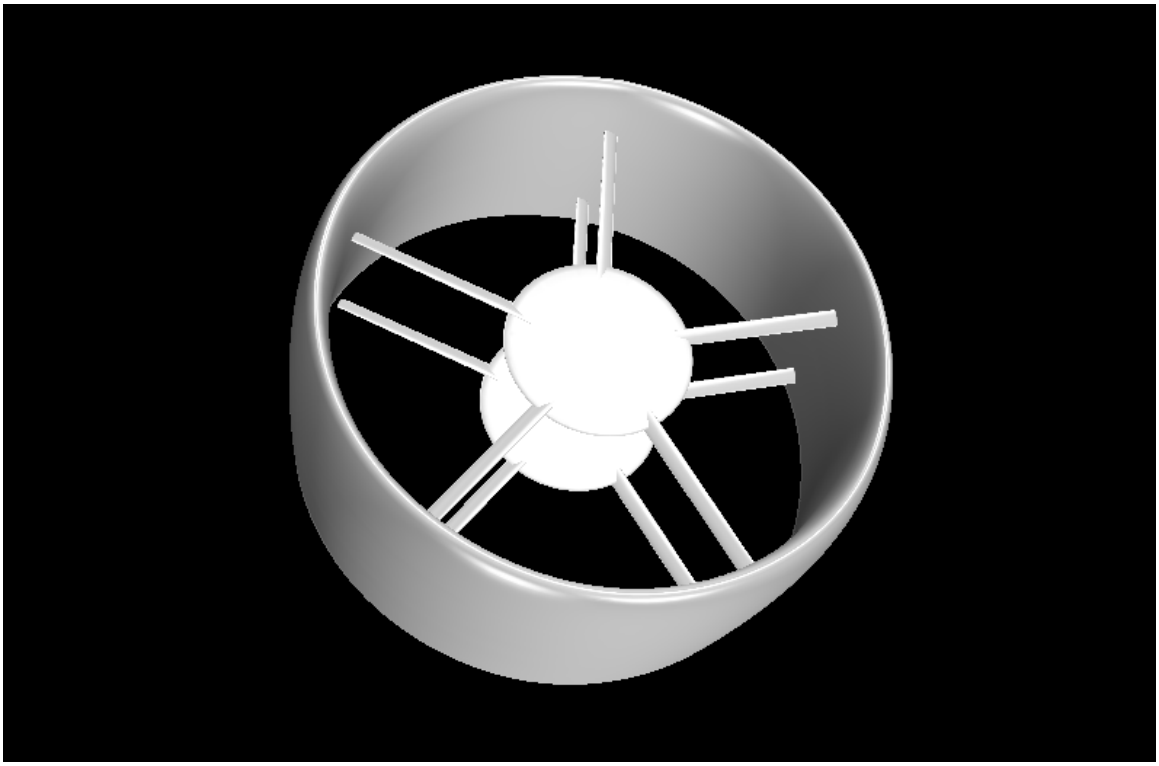

Figure 4.3: *Both* case 1 geometry

4.2 CFD

All CFD work was done using the commercial CFD package Star-CCM+. In order to obtain an accurate acoustic signature of these complex configurations, an accurate flow field must be obtained. Unfortunately, this project did not have the scope for complete accuracy, but the completeness of the flow field is important to the results that would be yielded. This means that there is a threshold for the amount of detail that is required for the investigated vehicles as well as a threshold for the scope of the computational expenses of the project. Due to processing and memory power available, there were computational limitations towards mesh size and run time per case.

This work is focused on a methodology and, therefore, an in depth analysis on the aerodynamics of each configuration is not looked at. A sensitivity study for the mesh was not done.

Since there was such a large number of cases needed to be run along with a large computational necessity, the batches of cases were created parametrically to automate the process as much as possible. A script was written to generate the Star-CCM+ files for each set of cases with parameters of interest being varied as needed. Star-CCM+ has a built in java macro capability; therefore, one simulation was created with a java macro that was then varied for the other runs parametrically. The java macro was altered using a Matlab script for each of the significant parameters. This capability pulls in the geometry, sets up regions and domains, meshes the system and applies physics and flow conditions without need for user input.

4.2.1 Domains

This research utilized rotating body domains in order to isolate rotation on the rotor (not include the duct). Cylinders were created for each rotor depending on the case. For the coaxial case and the *both* case, two cylinders were used, while in the ducted case only one

cylinder was used. The motion specification was defined based off of the RPM desired for each case individually. This method is found in Cornelius's paper and the Star-CCM+ user guide [42] [43] [44]. A rectangular box was used to encompass the whole system to represent a free stream region. Walls of the box were used to define the inlet, outlet, and symmetric wall. The box was adjusted based on the size of the rotor and duct, where relevant, along with computational limitation. An internal interface was used to join the regions of the cylinders and the box since they have the same medium. This is displayed in Figures 4.4 through 4.6.

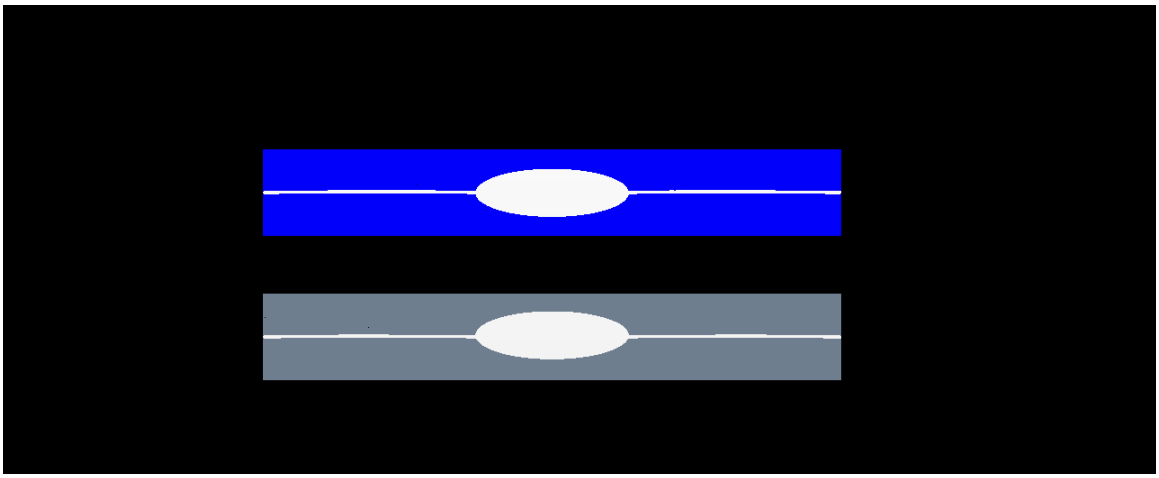

Figure 4.4: Coaxial case 1 domains

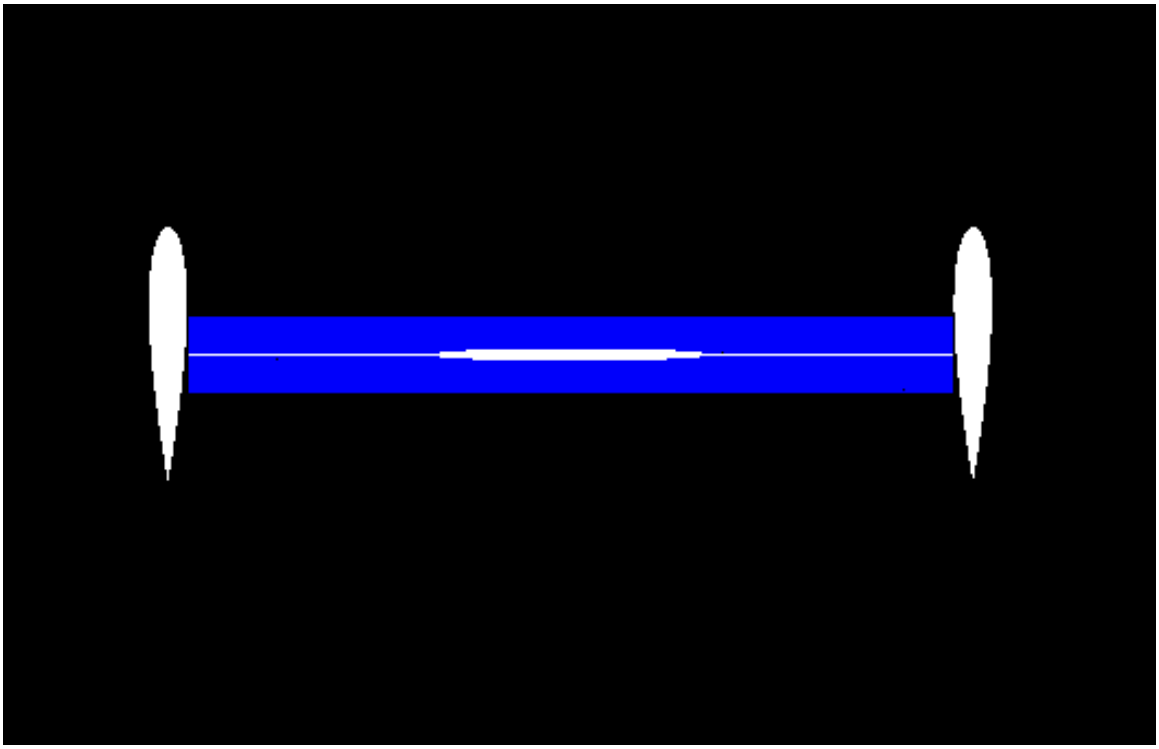

Figure 4.5: Ducted case 1 domains

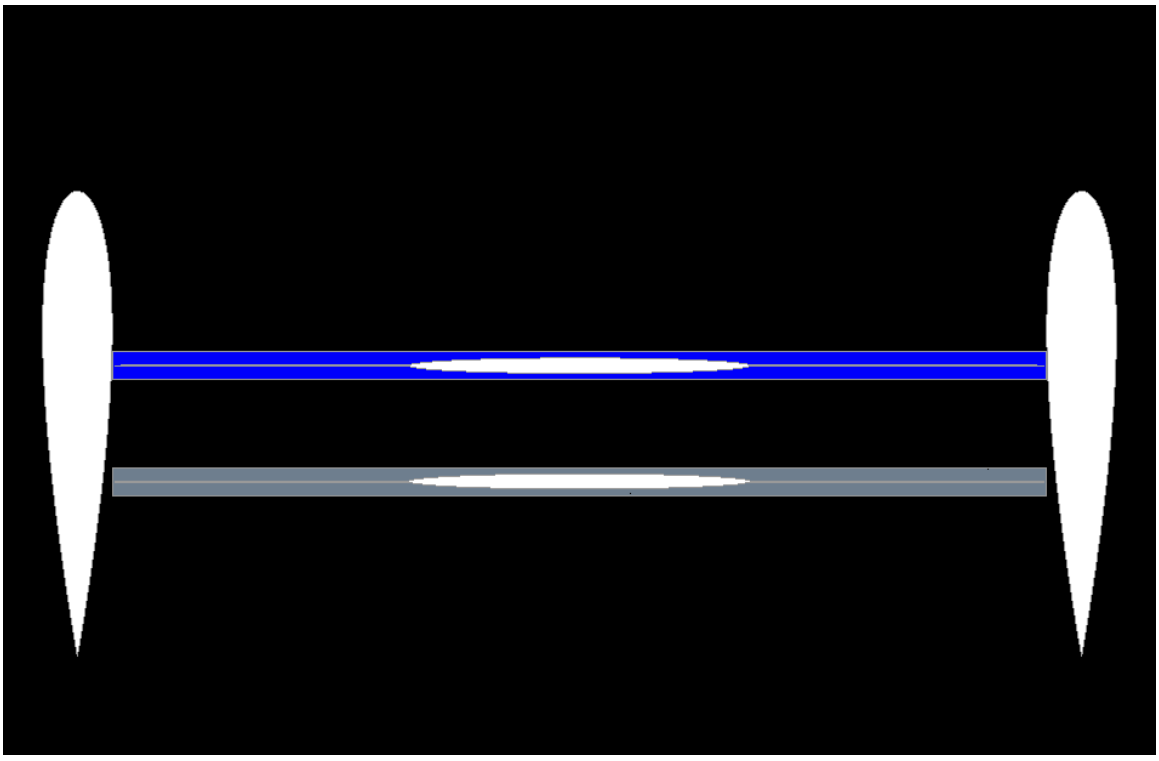

Figure 4.6: *Both* case 1 domains

4.2.2 Mesh

Star-CCM+ has options that allow for either structured or unstructured meshing. For this research, an unstructured mesh was utilized so that a finer grid could be more defined in more significant areas, while saving computational time in less important areas, such as farther away from the system.

When using CFD for aeroacoustic applications, a trimmed mesh is generally suggested because it provides the least amount of dissipation for flow disruptions. This comes at the cost of lower accuracy, due to the 1:2 mesh size transitions which may produce internal wave reflections. Polyhedral meshes are more accurate and provide smoother mesh size transitions at the cost of being more dissipating[45]. A polyhedral mesh was used for the system because it was more accurate and gave a denser mesh than a trimmed mesh. This was preferred for the more complex three-dimensional geometry that is being analyzed.

The mesh varies for each case. A mesh sensitivity study was not done for this research. A suitable mesh was found for a single run within a batch of cases and based on the base size and other parameters with respect to geometry size, it was scaled appropriately for other runs based off rotor radius and the gap between rotor and the duct. The convergence criteria was determined through a decrease in the magnitude of the residuals to about $10^{-}3$. Two surface wrappers were used to refine the tessellation of the geometry, which helps to fill any potential holes in the surface. Figures 4.7 through 4.9 show exemplary meshes for the three batches of cases used.

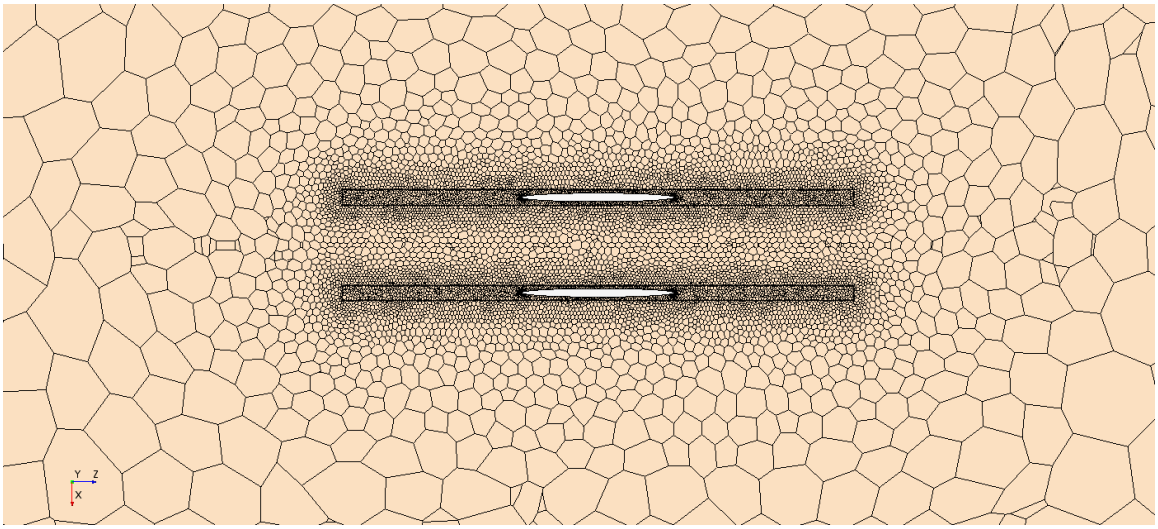

Figure 4.7: Coaxial case 1 exemplary mesh

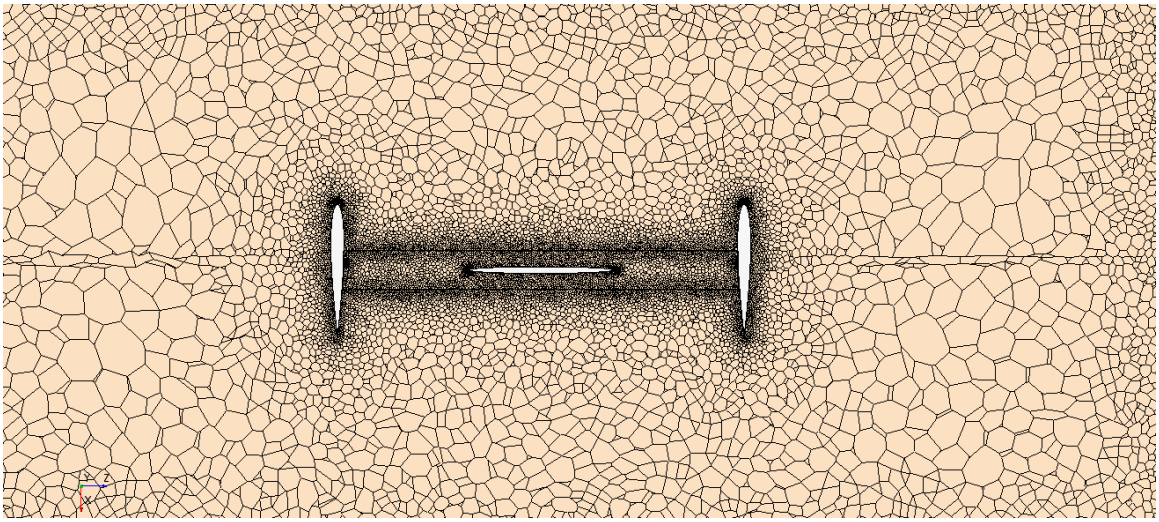

Figure 4.8: Ducted case 1 exemplary mesh

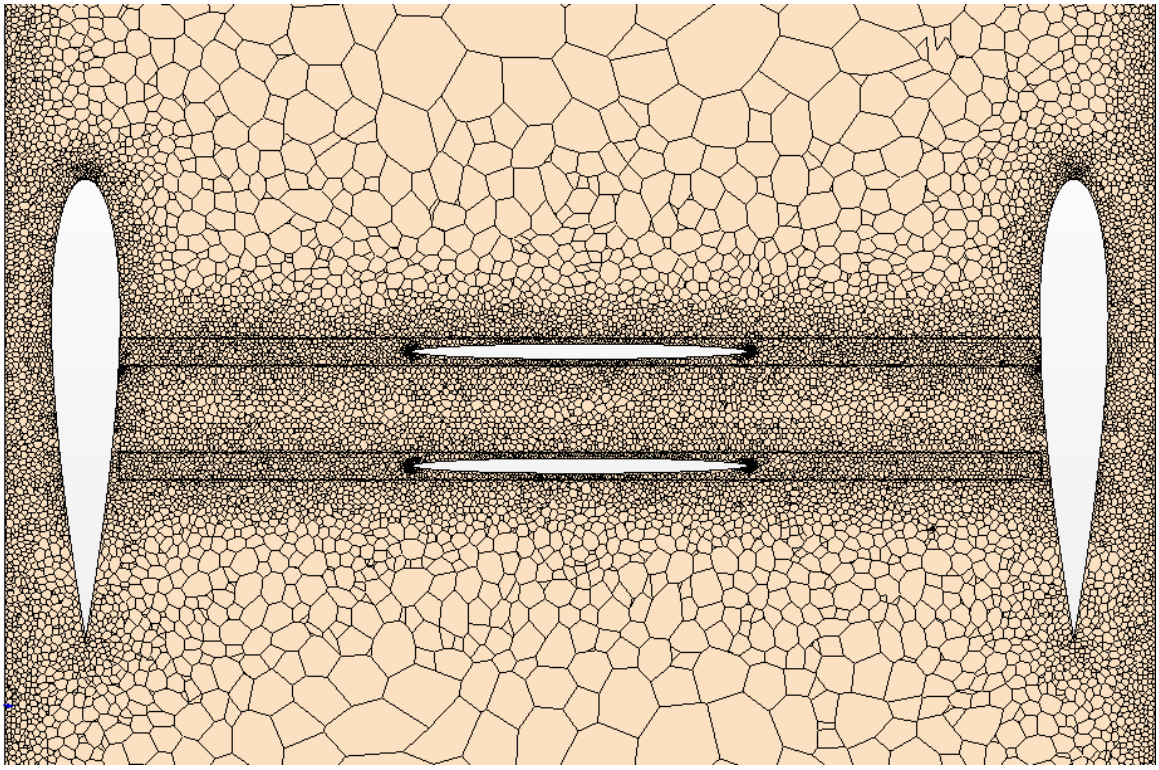

Figure 4.9: *Both* case 1 exemplary mesh

4.2.3 Physics and Flow Conditions

CFD can be used to capture various types of flow. Particular settings and physics models are needed in order to properly capture the acoustics within this system. Modeling of unsteady and turbulent flow is needed in order to account for any uncertainty within the flow. Turbulent flow is necessary for the broadband component. The flight conditions are taken from the literature review and stated in Table 4.2 [1].

Unsteady Reynolds-averaged Navier-Stokes is not recommended for aeroacoustic application because it cannot fully capture the turbulent qualities of the flow, which is important for broadband noise [46]. Large-Eddy Simulation (LES) is more computationally expensive than Detached Eddy Simulation (DES) in cases where boundary layers are resolved. For wall bounded, high Reynolds number flow, it is recommended to use DES [45]. DES is a hybrid approach using aspects of both LES and RANS solvers where boundary layers and irrotational flow regions use a base RANS model, while the turbulent aspects use

a LES model where the mesh is fine enough [47]. DES was chosen for the physics condition for this research as it was shown to fully encompass the flow needed to calculate the full spectrum of noise. Within the DES model the Spalart-Allmaras was further specified. This was to due to importance of the magnitudes of the relevant quantities (acoustic pressure, density, and velocity fluctuation) which can be very small in comparison to hydrodynamic quantities. Within aeroacoustics the magnitude of acoustic pressure fluctuations are often on the order of .01 of a Pascal [47].

Time step had to be adjusted based on the convergence of the mesh for some of the more condensed geometry configurations. The smaller the time step, the longer the simulations take to run. This was attempted to be minimally changed as to keep consistency across all runs and to maximize run time efficiency.

The number of iterations chosen for this research was based off of the residuals decreasing enough and computational limitations. The residuals for all cases were accepted if shown to have convergence.

Table 4.1: Atmospheric conditions for CFD

Variable	Value	Unit
Pressure	2118.17	(lb_f/ft^2)
Viscosity	$3.737x10^{-7}$ (viscous)	(slug/(s-ft))
Density	0.002377	($slug/ft^3$)
Temperature	518.7	(R°)
Speed of Sound	1116.46	(ft/s)

Table 4.2: Physics and boundary conditions for CFD

Flow	Implicit Unsteady
	Coupled Flow
	Turbulent
Turbulence Model	Spalart-Allmaras Detached Eddy
Mesh	Polyhedral (with surface remesher)
Boundary Conditions	Inlet = Velocity Inlet
	Outlet = Pressure Outlet
	Cylinder = Wall (with interfaces)
	Block Faces = Symmetry Plane

CHAPTER 5
ACOUSTIC SOLVER

PSU-WOPWOP allows use of the Ffwocs William Hawking equation in its most convenient form. This form of acoustic solver gives the most accurate results with as minimum time constraints to fit the scope of the experiment. An acoustic solver such as CAA would be too computationally expensive, but give the most accurate results. Other acoustic solvers such as the ones built in CFD like Star-CCM, or Ansys Fluent would not give the level of fidelity that is desired. Semi-empirical acoustic model allow for too many uncertainties to provide the confidence necessary to deliver accurate results.

There are some limitations to using PSU-WOPWOP. It is important to note that noise scattering results are not part of PSU-WOPWOP capabilities. This may impact the results of the duct case, especially. Broadband noise was not included in this experiment, even though PSU-WOPWOP has this ability and also may impact the results.

5.1 Inputs into PSU-WOPWOP

PSU-WOPWOP uses as many inputs as it is given which includes geometry, loading, and broadband. A namelist file denotes the number of rotors and blades, location of files, observers, and the desired outputs.

For this particular situation, it is desired to model thickness and loading noise. Since the regime of interest is subsonic flow, noise phenomena in the supersonic regime will be ignored.

Geometry files are generated within a Matlab script where an airfoil is denoted by the various parameters within the run matrices (Figures 2.1 to 2.3) along the defined span locations. Using the equation for a symmetrical four digit NACA airfoil and using the airfoil thickness, Cartesian coordinates are generated. The coordinates are then scaled

at each span location based on the chord and taper ratio, rotated by the twist, and then converted into a matrix. The final geometry file is a tuple representing a single rotor blade.

PSU-WOPWOP requires a geometry file for each blade in the rotor. Since each blade has the same design in the rotor, only one geometry file is needed to define each of the blades. Within the namelist file, the number of rotors and number of blades is denoted in reference to the geometry file and repeated as needed.

The loading files for PSU-WOPWOP require the forces on the blades. Star-CCM+ exports pressure and area which are converted to forces. A Matlab script is then used to create the loading file. Design parameters (such as geometry and rotational speed) are fed into the code in order to distribute the forces across revolution of the blade spinning around. This gives the loading its periodic nature.

A single point receiver will be placed at around fifteen degrees clockwise to the plane of the rotor. This is done to include both thickness and loading noise. If the observer was placed directly underneath the rotor, there may be no thickness noise present due to the directivity of thickness noise. Figure 5.1 shows a representation of the observer location. This was chosen to match some of Schatzman's observer locations [1].

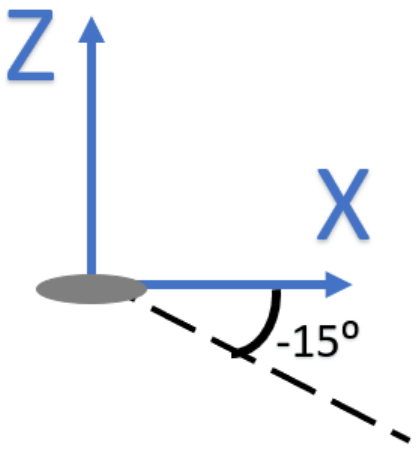

Figure 5.1: Observer location in PSU-WOPWOP

Surface pressures from Star CCM+ were exported in a tecplot format where a python and Matlab script was used to reformat the data into a readable format for PSU-WOPWOP.

5.2 Outputs of PSU-WOPWOP

PSU-WOPWOP can output several files, but for this study, the most concerning are the OASPL values, acoustic pressure, and the frequency spectrum. There is an OASPL for thickness noise, loading noise, and total noise. Other outputs can be specified within the namelist file depending on the noise metrics that are desired for the study.

The benefit of using PSU-WOPWOP and its use of Ffowcs Williams Hawkings equation is that the noise is broken out from total noise into both thickness and loading noise separately.

CHAPTER 6

RESULTS

6.1 CFD Results

The CFD from this study provides the surface pressures on the blade, as well as providing insight on Mach number. Fluid flow over time was not investigated during this study due to computational time and expenses. Also since the flight condition remains at hover, it is assumed that the CFD will reach a point of consistency. Within the screening test DOE, there is a single case where all the parameters match across configurations. The following cases show all the parameters referenced in 2.1 through 2.3 at their midpoint.

Blade tip Mach number allows us to confirm the speed of the blade with the speed intended from the run matrices. Figures 6.2 through 6.4 show the blade tip Mach number contour for the cases that match across all configurations. The Mach number is shown to be highest across all cases at the blade tip which matches the run matrices and supports the integrity of the experiment. Vortices disperse outward away from the blade following the trailing edge. Within the *both* case (Figure 6.4) the vortex is much more contained compared to the other configurations. This could be due to the containment of the duct on the configuration or due to the low fidelity of the CFD being unable to capture the dispersion.

Since Schatzman's work investigated a coaxial rotor system, the flight conditions were chosen to match that of her work (See Table 4.2). It is expected to see results within similar magnitude to her work. It should be noted Schatzman experiment is completed in 2D with a fully converging mesh, and using different software programs resulting in differences in outputs.

Figure 6.2 shows similar magnitude at the leading and trailing edges, of Schatzman's

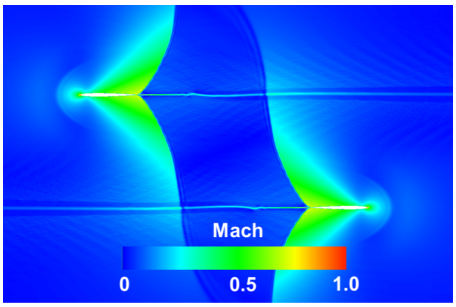

Figure 6.1: Mach contour of a 2D coaxial rotor [1]

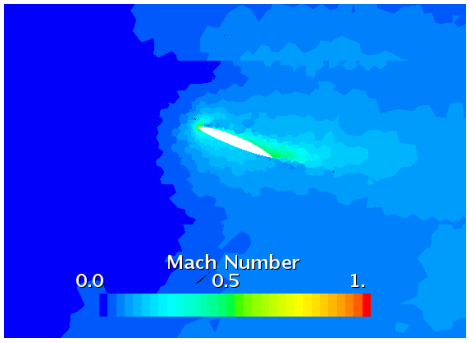

Figure 6.2: Blade tip Mach number contour for coaxial case 1

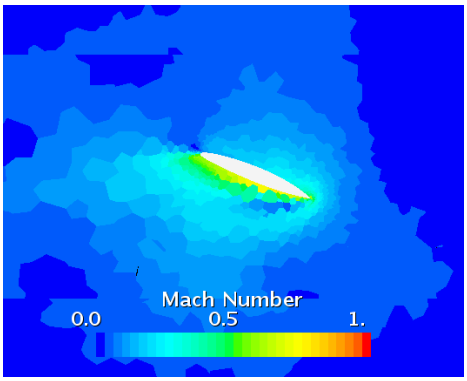

Figure 6.3: Blade tip Mach number contour for duct case 1

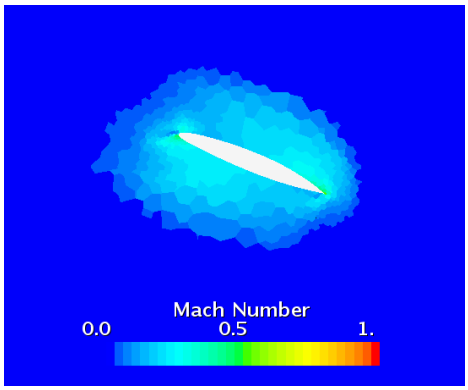

Figure 6.4: Blade tip Mach number contour for *both* case 1

work, seen in Figure 6.1. This helps to verify the results for the CFD process used[1]. Even though the configurations between Schatzman and this work are the same, the design parameters vary such as vertical separation. Her work does not use any blade twist and looks at the crossing of two blades, two dimensionally and mirrors it. Figure 6.2 shows a five bladed rotor with a blade twist of seven and a half in three dimensions.

The shape of the contour varies a good amount from Schatzman's, this is probably due to the fact there is not as much refinement in this study's cases, as well as the vertical separation is much larger. Schatzman did a more in depth investigation into coaxial rotors, while this experiment focuses on the parametric study of inputs. Therefore validation of the CFD cases are not the primary focus.

The most important data that is coming from the CFD is the surface pressures on the

blades. This pressure is the static gauge pressure and is in reference to the atmospheric pressure.

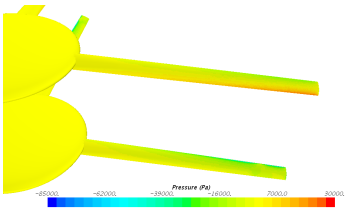

Figure 6.5: Pressure contour isometric view of coaxial case 1

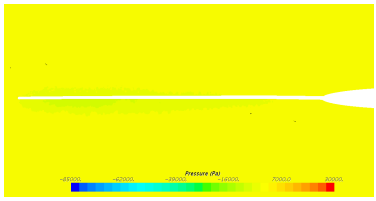

Figure 6.6: Pressure contour side view of coaxial case 1

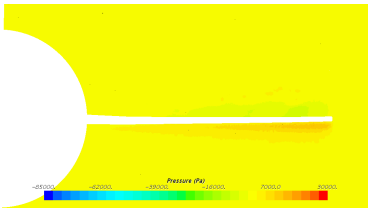

Figure 6.7: Pressure contour top view of coaxial case 1

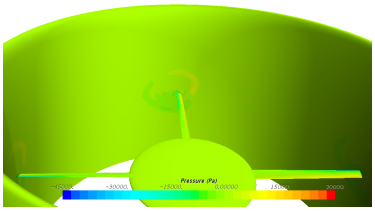

Figure 6.8: Pressure contour isometric view of duct case 1

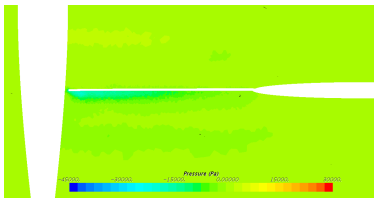

Figure 6.9: Pressure contour side view of duct case 1

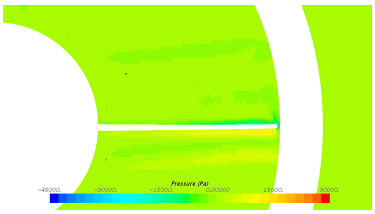

Figure 6.10: Pressure contour top view of duct case 1

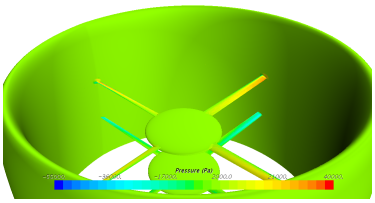

Figure 6.11: Pressure contour isometric view of *both* case 1

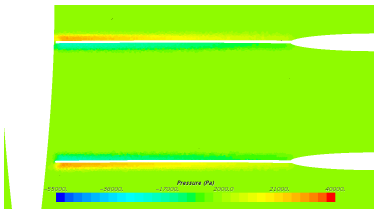

Figure 6.12: Pressure contour side view of *both* case 1

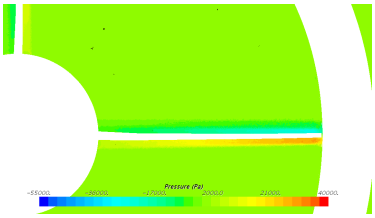

Figure 6.13: Pressure contour top view of *both* case 1

6.2 PSU-WOPWOP Results

The primary results of PSU-WOPWOP important for this study are the observer file, which contains the OASPL values, and the frequency spectrum. The OASPL values are the single point measurement for how loud the vehicle is overall. The numbers are fed into JMP to help build the representative noise model. Looking at these values across the run matrices

may not necessarily show obvious trends because the screening test displays a spread of the data over various parameters. Therefore, there may be too many parameters changing at once to be able to see a clear trend across the run matrices with the OASPL values.

It is important to note that due to the DOE, each case has varying parameters that may not easily match throughout configurations. Comparisons can only be made when there are limited independent factors, otherwise results would be convulted with so many varying parameters. Majority of the comparisons can only be made within a single configuration. There is one case across all three configurations in which all the variables are the same. Within this case seen in Table 6.1, is where conclusions across configurations are drawn. It is recommended that more cases are done with matching parameters to confirm these results. The coaxial case and *both* case are within 0.02 of a decibel of each other, while the ducted case is noticeably lower. It can be said that the addition of a duct does not counteract or impact the noise from the additional rotors.

Table 6.1: OASPL for matching cases across all configurations

Configuration	OSAPL (dB re: 20 micro pascals)
Coaxial Case 1	102.31
Ducted Case 1	95.85
Both Case 1	102.33

The results below come with some limitations and understandings. Rotor noise is very directional in nature as shown in the literature review. The location of the observer angle is important to keep in mind. Results may vary largely with a different observer angle. As the observer angle moves closer to directly under the rotor, thickness noise would be lessened. The other dependency that impacts the results are the ranges chosen for each parameter. The outputs given are directly linked to how much each parameter was allowed to vary.

With different ranges, the significant parameter orders may be very different.

6.2.1 Frequency

The frequency of noise determines a large part of the community annoyance or acceptance of the noise, along with other factors which would be better analyzed by a pyschoacoustic study. This gives insight into the human perception of these vehicles.

Frequency spectrum was compared across cases in which the geometry matched as well as with a case that matched speed (in order to match RPM and BPF), but varied in some geometry. The left hand side of the figures below (Figures 6.14, 6.16, 6.18) match across geometry and CFD conditions for a configuration comparison and the right side figures (Figures 6.15, 6.17, 6.19) are the corresponding configuration and CFD condition, with different design parameters.

PSU-WOPWOP breaks out the noise in three parts: thickness, loading, and total noise. This helps to locate design parameters that may be causing the noise directly. In all the cases, thickness overlaps almost completely with total noise, which seemingly dominates even in the ducted cases. This observation that thickness noise dominates, primarily in the coaxial cases, matches Schatzman's work in her paper, which continues to validate the study. The frequency shape across case one is consistent across all configurations. The noise level is lowest for the duct configuration which is reasonable when looking at the physics of the system. Since thickness noise is the largest source of noise, it is sensible that the configuration with the least amount of rotor blades would be the quietest. Along with considering the blockage the duct does to reduce noise. The peak frequency within case one happens around 38Hz, which is in the human range of hearing. Looking at the first cases against the comparison cases there is a high spike compared to a smaller wider incline. This could change the human response of the system significantly.

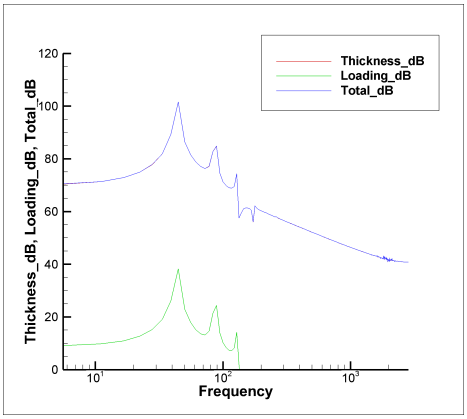

Figure 6.14: Frequency spectrum for coaxial case 1

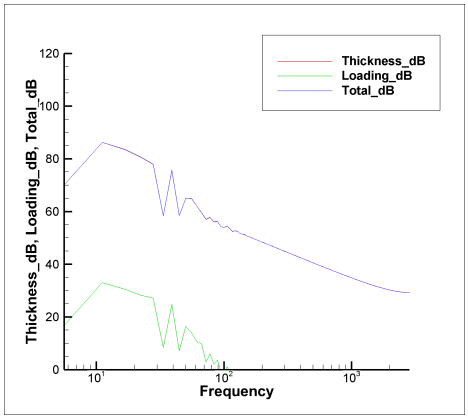

Figure 6.15: Frequency spectrum for coaxial case 6

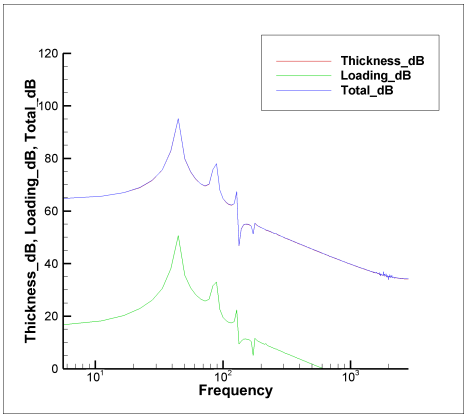

Figure 6.16: Frequency spectrum for duct case 1

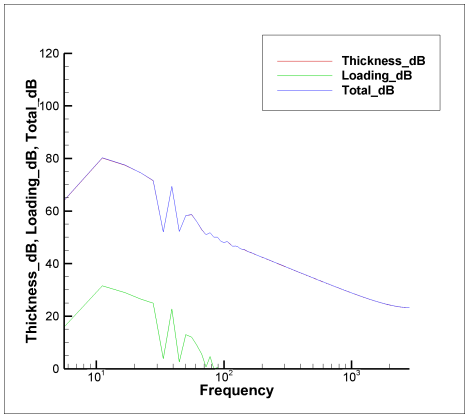

Figure 6.17: Frequency spectrum for duct case 8

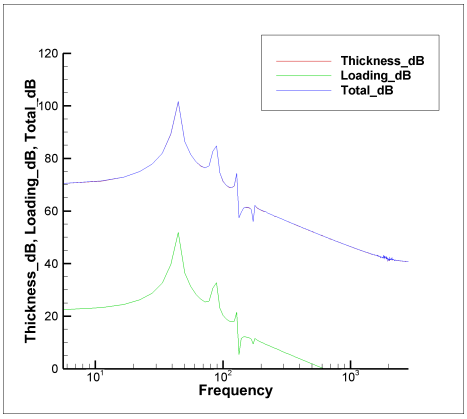

Figure 6.18: Frequency spectrum for *both* case 1

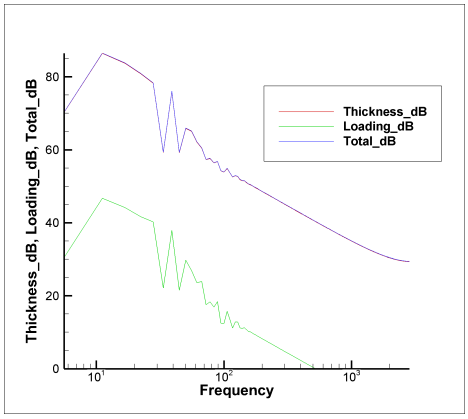

Figure 6.19: Frequency spectrum for *both* case 9

6.3 Data Analysis and Model Generation

The following sections details influential parameters, analyzing trends, and several different model fits to the data. The data did show one outlier when generating the model fits and therefore that outlier was excluded and model fits were rerun for improvement. An outlier can happen if the level of fidelity of the CFD was not refined enough. The outlier was consistent across all three cases. Overall, the majority of the data aligns with several trends and the experiment is acceptable.

6.3.1 Influential Parameters

The varying inputs and the resulting outputs were inputted into JMP bootstrap forest partitioning predictor screening test. This allows for quantifying how influential parameters are to the results. The top 80 percent of contributors are considered significant, but this does not determine if these parameters are negatively or positively significant.

The coaxial configuration influential parameters show the design parameters being much more significant compared to the configuration parameter of vertical separation. Vertical separation borders the line of top 80 percent of significant parameters. This is seen in Figure 6.20.

Predictor Screening

	OASPL			
Predictor	Contribution	Portion		Rank
Blade Tip Mach Number	295.504	0.3864		1
Chord	126.151	0.1649		2
Rotor Radius	102.514	0.1340		3
Blade Twist	65.457	0.0856		4
Vertical Separation	53.655	0.0702		5
Number of Blades	48.325	0.0632		6
Taper Ratio	42.171	0.0551		7
Airfoil Thickness	31.074	0.0406		8

Figure 6.20: Influential parameters by percentage for coaxial cases

Figure 6.21 show the influential parameters from the duct configuration. The vehicle design parameters, such as blade tip Mach number and rotor radius remain the most significant, while the configuration parameters are near the bottom. The cut off for the significant influential parameters is right after airfoil thickness. This means that the configuration parameters are considered insignificant to noise along with number of blades and taper ratio.

Predictor Screening

	OASPL			
Predictor	Contribution	Portion		Rank
Blade Tip Mach Number	266.847	0.2667		1
Rotor Radius	200.466	0.2004		2
Chord	148.057	0.1480		3
Blade Twist	122.629	0.1226		4
Airfoil Thickness	63.766	0.0637		5
Duct Thickness	58.722	0.0587		6
Duct Width	51.399	0.0514		7
Number of Blades	46.382	0.0464		8
Taper Ratio	42.256	0.0422		9

Figure 6.21: Influential parameters by percentage for ducted cases

The *both* configuration influential parameters, seen in Figure 6.22 show the configuration specific parameters as less significant compared to the general vehicle design parameters. The airfoil specific parameters are more dispersed in their influential value. Duct thickness borders the line of the top 80 percent of significant parameters while the other configuration parameters are considered insignificant to noise. Airfoil thickness and blade twist are just a few of the design parameters that are also considered insignificant to the results.

Predictor Screening

	OASPL		
Predictor	**Contribution**	**Portion**	**Rank**
Blade Tip Mach Number	349.316	0.2226	1
Chord	291.428	0.1857	2
Rotor Radius	214.735	0.1369	3
Number of Blades	194.094	0.1237	4
Taper Ratio	126.259	0.0805	5
Duct Thickness	104.462	0.0666	6
Airfoil Thickness	95.696	0.0610	7
Blade Twist	81.254	0.0518	8
Duct Width	71.246	0.0454	9
Vertical Separation	40.591	0.0259	10

Figure 6.22: Influential parameters by percentage for *both* cases

6.3.2 Identifying Trends

Identifying trends can be done within each configuration and also across all three. Since the parameters change across each configuration, there are limited ways in which comparisons can be made. By listing the most influential parameters across the board, trends can be seen and analyzed.

Influential Parameters	Coaxial Cases	Ducted Cases	Both Cases
1st Influential	Blade Tip Mach Number	Blade Tip Mach Number	Blade Tip Mach Number
2nd Influential	Chord	Rotor Radius	Chord
3rd Influential	Rotor Radius	Chord	Rotor Radius
4th Influential	Blade Twist	Blade Twist	Number of Blades
5th Influential	Vertical Separation	Airfoil Thickness	Taper Ratio
6th Influential	Number of Blades	Duct Thickness	Duct Thickness
7th Influential	Taper Ratio	Duct Width	Airfoil Thickness
8th Influential	Airfoil Thickness	Number of Blades	Blade Twist
9th Influential	N/A	Taper Ratio	Duct Width
10th Influential	N/A	N/A	Separation

Figure 6.23: Influential parameters across configurations

Looking at the influential parameters across all three configurations, it is shown that blade tip Mach number remains the most influential parameters, which is logical considering the physical relationship between speed and volume. This validates the experiment, by confirming the relationship. Rotor radius and chord length become the next influential parameters across all three cases, which defines how large the vehicle and the blades are, making them unsurprisingly top influential parameters. The fact that the top three parameters are the same across all configurations, make it reasonable that there is a potential for a high correlation between configurations.

By the fourth parameter, there starts to be some differences between the configurations, but still the design parameters remain more influential than the more specific configuration parameters. This means that the configuration of the vehicle may not be as important as the rotor design itself.

6.3.3 Representative Model

Multiple types of regression are attempted to fit the data. This is to look at what may be the best fitting model. Neural networks (with multiple layers), fit of least squares, and stepwise regression models are all attempted and discussed here.

There are many representative models that can be employed, but it is important to compare the quality of these models. The fit of these models can be quantified in multiple

ways; for overall fit the R squared value will be of primary interest. An R squared of one represents a perfect positive correlation between the data and the model. These models are all created using JMP and are summarized in Figure 6.24.

There are are several graphs displayed for each model that is used to help characterize the fit of the model to the data. An actual by predicted plot displays the actual data points against the line from the model. It is desired for a good spread of the data across the model line, while staying as close to the line as possible. Clumping within these graphs can show that a particular variable is driving the response. A ”bad” fitting model would have data points scattered too far away from the model fit line. While the residual by predicted plots show the error in the fitted model. If a model has a ”good fit” the residual vs predicted plot is scattered and random centered about zero to show that neglected higher order terms and effects are negligible.

Each model includes a model profiler which displays the impact of each parameter on the model. The profilers are different than Figures 6.20 to 6.21 because the profiler shows how influential the particular parameters that are used in the models are to the model itself. These give more detail by showing at what point the parameters have a negative impact to the output. The model may not include certain parameters if it allows for a better fit of the data. Figures 6.20 to 6.22 include the influence of all the parameters to the results, but not whether or not that impact is negative or positive.

Configuration	Surrogate	Set Used	R Square
Coaxial	Neural Net	Training	0.66
		Validation	0.91
Duct	Neural Net	Training	0.99
		Validation	0.95
Both	Neural Net	Training	0.96
		Validation	0.96
Coaxial	Fit of Least Squares	N/A	0.87
Duct	Fit of Least Squares	N/A	0.95
Both	Fit of Least Squares	N/A	0.93
Coaxial	Stepwise Regression	N/A	1
Duct	Stepwise Regression	N/A	1
Both	Stepwise Regression	N/A	1

Figure 6.24: Summary of representative models

6.3.3 Neural Net Model

Neural net models, allow for layering when it comes to number of terms allowed into the models. The model divides up the data that is given into training and validation data. This can be tricky to compare because the validation data and numbers can be more important than the training data. The validation data is best thought of as a standard error to the training data; regardless of how well the training data fits, if the validation does not fit well than the entirety of the model does not fit well.

Neural networks can be generated with several different layer and function combinations. JMP provides several options of variations such as TanH layer, linear layer, holdback proportion, and number of tours. These all effect the model and fit the data in different ways. These model fits were done using three TanH layers, no linear layers, a holdback proportion of 25 percent, and three tours. Other layer variations were attempted. What is displayed is the best result.

6.3.3.1.1 Coaxial Cases Figure 6.25 displays a neural net model with three terms for the coaxial configuration cases. Overall the R squared value for the training data is pretty low at a .65, while the validation data is better at .9, but having a R squared value of one would be preferred. The actual by predicted plots show an even spread of data throughout for training points. There are not as many validation points to compare to, but seemingly distributed well. Residuals for this model look distributed fairly well, but with some gaps. There does not seem to be any large outliers within any of the plots within this section and, therefore, none of the data needs to be excluded at this point.

The profiler location near the bottom of the figure displays the sensitivity of the parameters to the results. The vertical separation shows an increase in OSAPL the farther the rotors are, but the influence is only minor. Rotor radius actually shows a more steady trend where the smaller the radius the louder the noise, while the larger the radius the quieter the noise. With blade tip mach number being the most influential parameter it makes sense that it displays one of the largest changes in the results. This relationship again confirms Figure 6.20 and the relationship between speed and volume. Number of blades shows an inverse relationship where the more blades there are, the quieter the vehicle is. This can be confusing to consider, since it would be presumed to have more interference noise the more blades. This may be due to the CFD not fully capturing interference noise. OSAPL shows a dependent relationship on chord size and blade twist. Finally, taper ratio and airfoil thickness do not seem to impact noise greatly in this configuration.

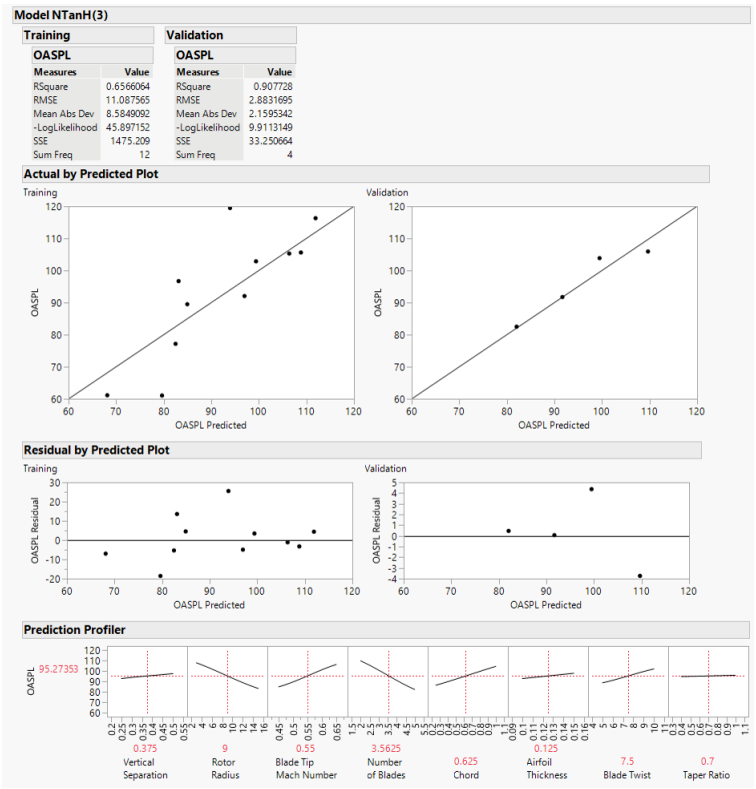

Figure 6.25: Neural net model for coaxial cases

6.3.3.1.2 Ducted Cases A neural net model with three terms for the duct configuration case is located in Figure 6.26. This model shows a much higher R squared value at .997, but a validation value of .79. The validation data is ultimately more important than the training data and therefore the model is not as accurate as is desired. There seems to be some clumping throughout the actual by predicted plot, which means there there are certain parameters that are driving the model development. The validation residual plot shows a clear line of the validation points and shows a pattern. The pattern and clumping of the various plots show that this model may not be the best.

The configuration parameters for the duct cases have a very little influence on the results within this neural network which align with the influential configuration parameters seen in Figure 6.21. Rotor radius shows a significant drop in noise around nine feet and continues lessening noise as rotor radius grows. This could be due to having more space for fluid flow, therefore less pressure fluctuations. Blade tip mach number and chord displays a negative

parabolic relationship to noise. These may be the driving parameters seen in the patterns in the previous graphs. Number of blades and airfoil thickness show a similar shape in response with a slight curve downward. Parameters that show very little response to noise are blade twist and taper ratio.

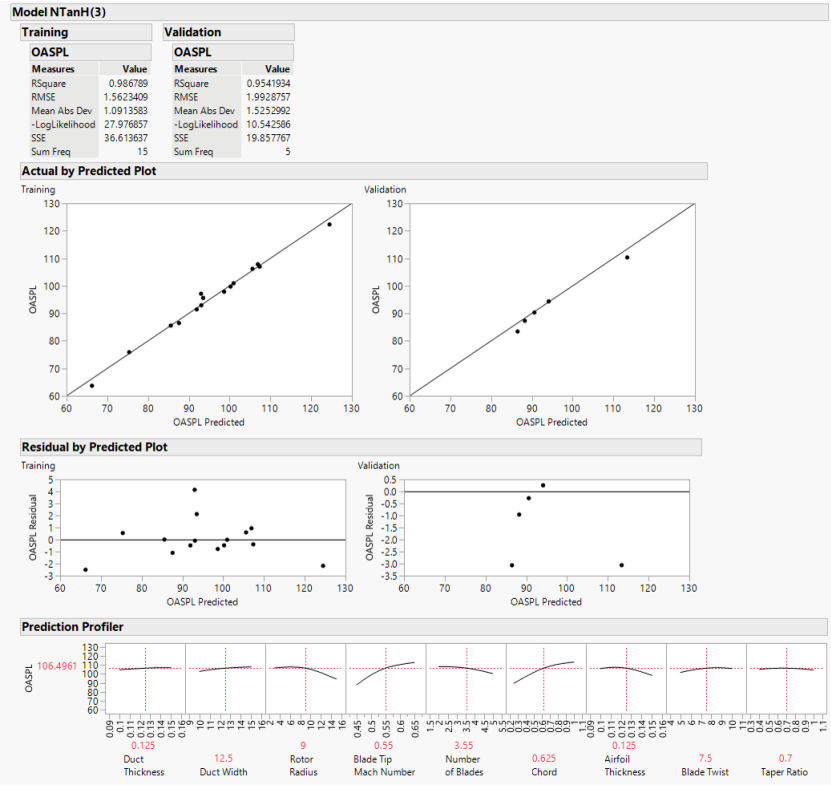

Figure 6.26: Neural net model for ducted cases

6.3.3.1.3 *Both* Cases Duct thickness, duct width, and vertical separation all remain to have very little impact on the results. Rotor radius and number of blades show to have an inverse relationship with noise within this model. It shows that the larger the rotor radius would allow for easier fluid flow and less noise. The greater the number of blades on a rotor results in less noise within this model.

Blade tip Mach number and chord have a large impact on the results, with a direct correlation between speed and noise. Airfoil thickness, blade twist, and taper ratio all have a direct correlation to noise in a less significant way than the previous mentioned parameters.

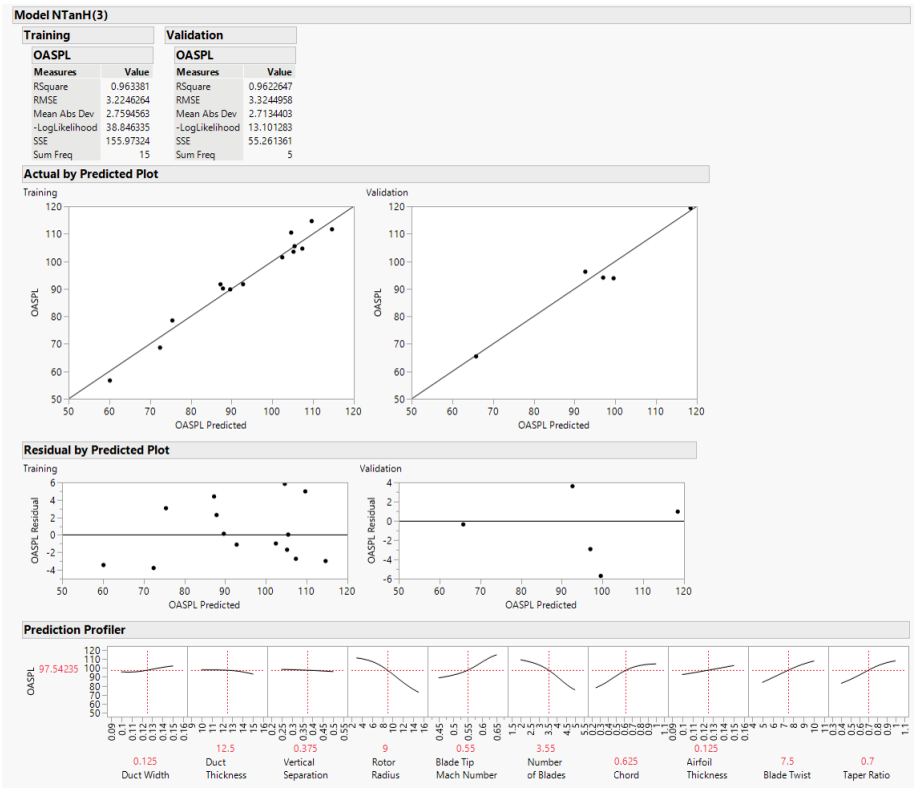

Figure 6.27: Neural net model for *both* cases

6.3.3 Least Squares Fit Model

Least square regression model is a second order response surface equation where the sum of square of the errors are minimized.

For this particular model type, the actual by predicted plots have a pink area shading which represents the 95 percent confidence intervals. A good fitting model would have these areas be relatively very small and close to the fit line.

The P value for each parameter shows the significance that parameter has to the model. If the value happens to be small, it shows that the parameter fits well inside of confidence intervals. This is another way to show an influential parameter's significance to the model.

6.3.3.2.1 Coaxial Cases The actual by predicted shows a wide display of standard deviation and data, showing that the model does not fit very well. There does not seem to be any outliers in the residual by predicted plot. The least squares fit model for the coaxial

cases shows an R squared value of .87, which is decent.

The parameter estimates are used to plot the prediction profiler, with the exact numbers and displays high values for standard deviation. The profiler for this model shows little impact to the results for vertical separation which matches 6.20. Blade tip mach number and chord, again, show a large impact and a direct relation to noise, with larger numbers resulting in more noise. While number of blades and rotor radius show an inverse relationship to noise. The other design parameters that relate to the smaller characteristics of the blade show little influence on the results in this model.

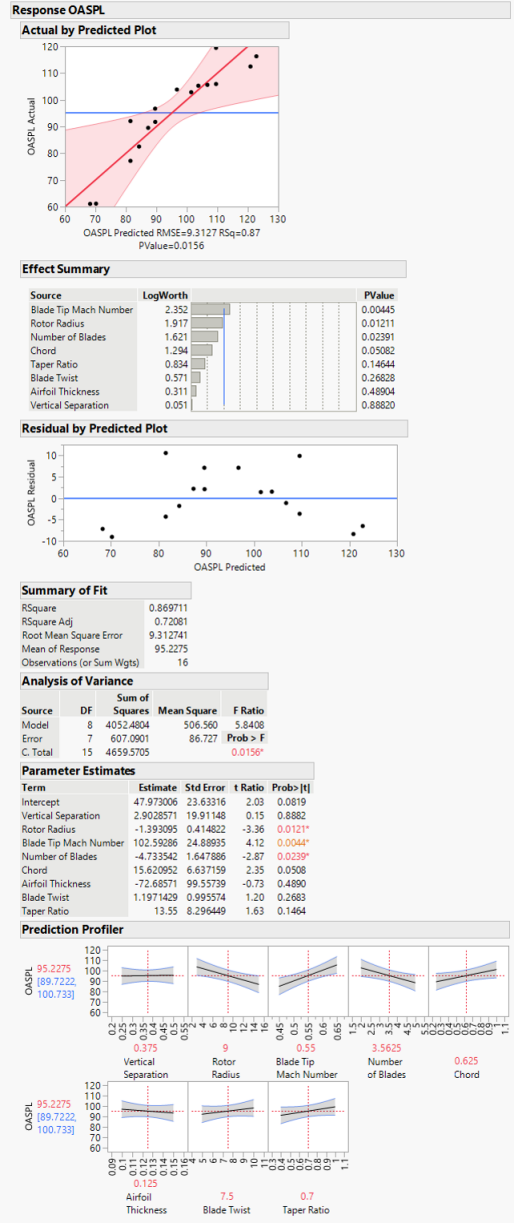

Figure 6.28: Least squares fit model for coaxial cases

6.3.3.2.2 Ducted Cases The least squares fit for ducted cases show a better stand deviation compared to the coaxial cases, but still there is a good amount of clumping. This show that one parameter is driving the model. There seems to be no clear patterns or outliers within the residual by predicted plot which shows a good fit for the model. The R squared value is much better than the coaxial cases at .94, seen in Figure 6.29.

This profiler displays much smaller standard deviation lines for each parameter com-

pared to the least squares fit model profiler for coaxial cases, that can be seen in the parameter estimates. This shows that this model is more accurate in comparison. The configuration parameters still show to have very little impact on the results. While blade tip Mach number and chord remain to be large drivers of noise with direct relationships. Rotor radius is also contributing to the results with an indirect relationship. Number of blades, airfoil thickness, blade twist and taper ratio do not appear to have a large influence on the results in this particular model.

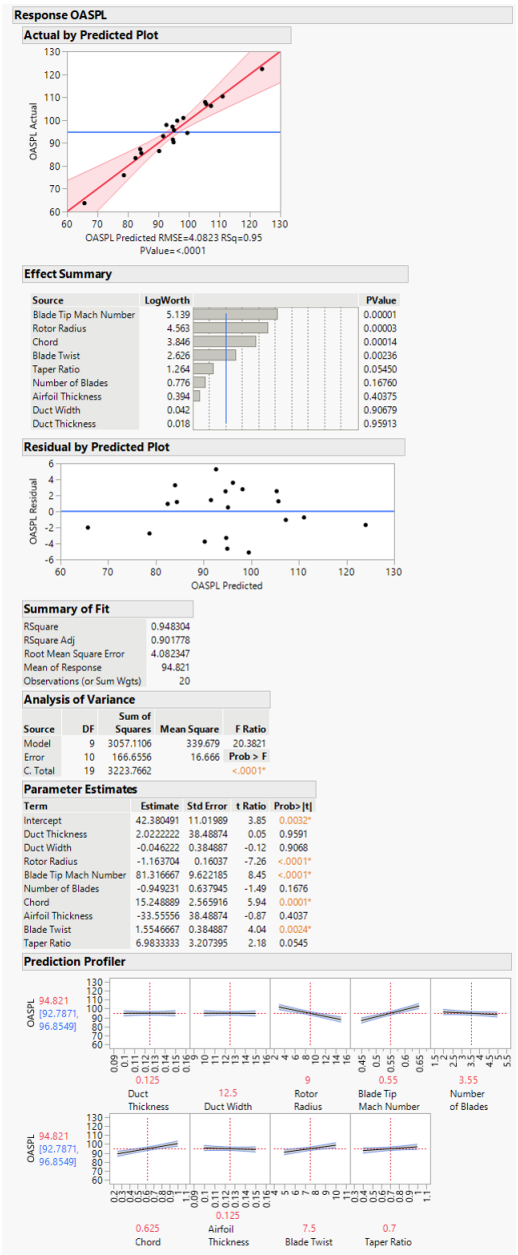

Figure 6.29: Least squares fit model for ducted cases

6.3.3.2.3 ***Both*** **Cases** Seen in Figure 6.30, the actual by predicted plot show a rather large standard deviation as well as a good amount of clumping of the data points. This shows that this fit is not very good with this data set. Within the effect summary, the P value for each of the parameters is smaller for the more influential parameters and larger for the less influential parameters.

There does not appear to be any outliers in the residual by predicted plot, but there is a good amount of clumping, showing that the model is being driven by certain parameters and not equally spread. There is a decent R squared value at .93.

The profiler for the *both* case configuration shows a standard deviation comparable to the the coaxial cases for the least squares fit model. The parameters within this model that show the largest impact are blade tip Mach number, rotor radius, number of blades, and and chord. Blade tip Mach number and chord display a direct relationship to the results allowing for more noise with greater speed or larger blades. Rotor radius and number of blades show an inverse relationship to noise, increasing with a smaller radius and fewer blades. The smaller design parameters such as airfoil thickness, blade twist, and taper ratio display very little impact on the results. These results remain consistent with the influential parameters in 6.22.

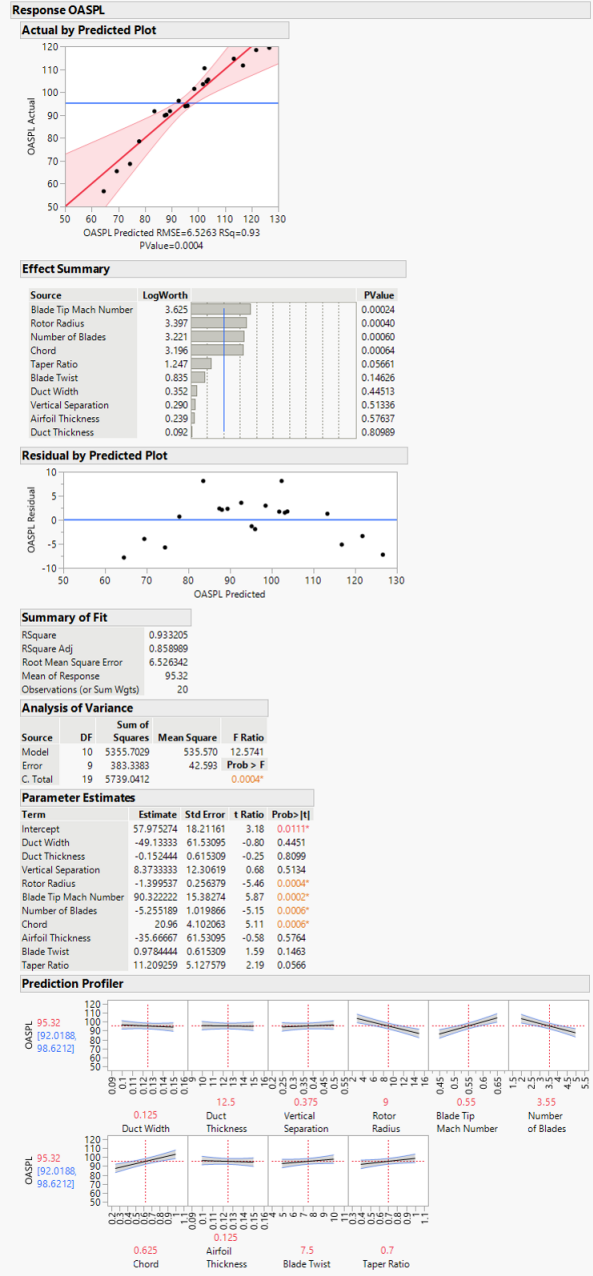

Figure 6.30: Least squares fit model for both cases

6.3.3 Stepwise Regression Model

The stepwise regression model uses an iterative process, creating a sequence of regression models by adding or removing variables. This means that not every parameter may be deemed as significant to the best fitting model.

Similar to the least squares fit model, the actual by predicted plot will have standard

deviation denoted in pink around the red model line. There will also be an effect summary displaying the P value for each of the parameters. When the P value is below a threshold (defined by a confidence interval), the parameter is significant to the model.

6.3.3.3.1 Coaxial Cases There is little standard deviation within the actual by predicted plot for the stepwise regression model for coaxial cases. This shows a good fit of the model to the data. The residuals by predicted plot show a good random scatter of the data. An R-squared value of one is the final indicator that the model is a perfect fit to the data. See Figure 6.31.

The parameter estimates and the profiler display very little standard deviation for the model, which proves positive for the experiment. Vertical separation still shows very little impact within the model, while rotor radius and number of blades both show a high impact and an inverse relationship. Parameters that have a positive relationship and a high impact in the model are blade tip Mach number and chord length. The remaining parameters are not major drivers of the results.

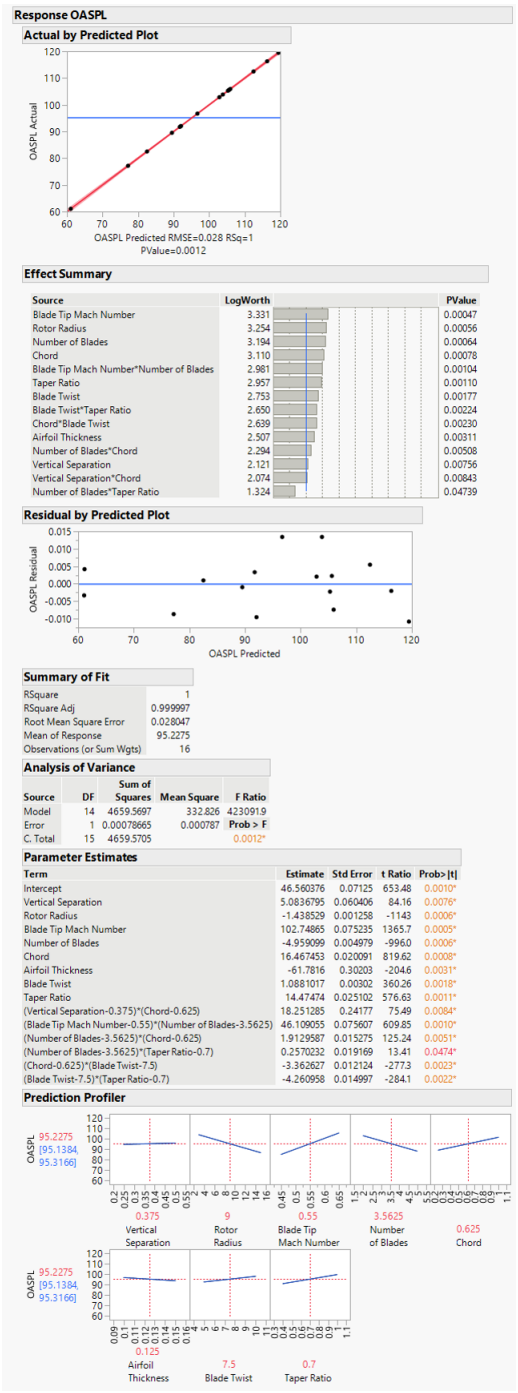

Figure 6.31: Stepwise regression model for coaxial cases

6.3.3.3.2 Ducted Cases The actual data plotted against the predicted results from the model show a good fit with little to no standard deviation. There is a pattern to the residuals, so this model may be driven by a single parameter, but the magnitude of the residuals are

rather small. The R-squared value for this model is a perfect correlation.

The configuration parameters were included in the model and still had little impact on the results. Blade tip Mach number was still a large driver of noise, with a direct relationship. Chord and blade twist also displayed a direct correlation to noise, with less contribution compared to blade tip Mach number. Rotor radius was the major driver of noise and had an inverse relationship, while other parameters did not show to have a large impact on the results the model still deemed them significant to the model generation. This is displayed in Figure 6.32.

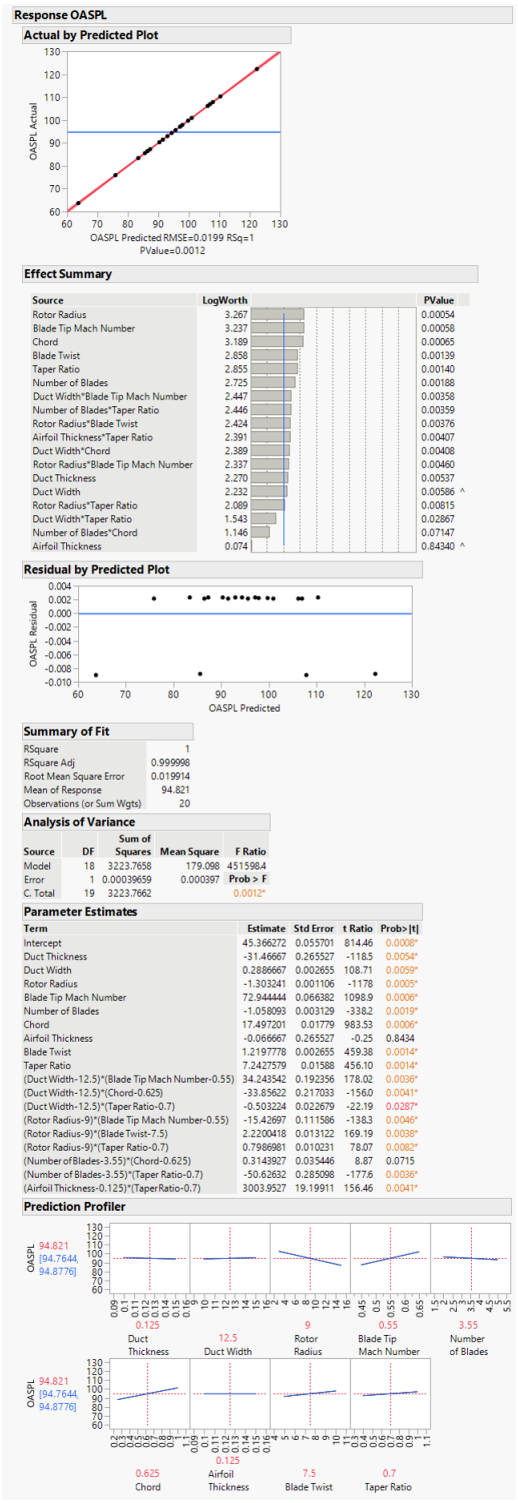

Figure 6.32: Stepwise regression model for ducted cases

6.3.3.3.3 *Both* Cases Shown in Figure 6.33, the actual by predicted plot shows very little standard deviation showing a good model fit. Within the residual by predicted plot there is a good scattering of the data. The R-squared value is the best it can be with a positive correlation of one.

Standard deviation on the profiler for the stepwise regression model for *both* cases remain small, showing the model is precise. The configuration parameters do not show a large impact on the results. Rotor radius displays a large impact on noise with an inverse relationship, while blade tip Mach number and chord length have a direct relationship. Airfoil thickness, number of blades, blade twist, and taper ratio show little impact on the results.

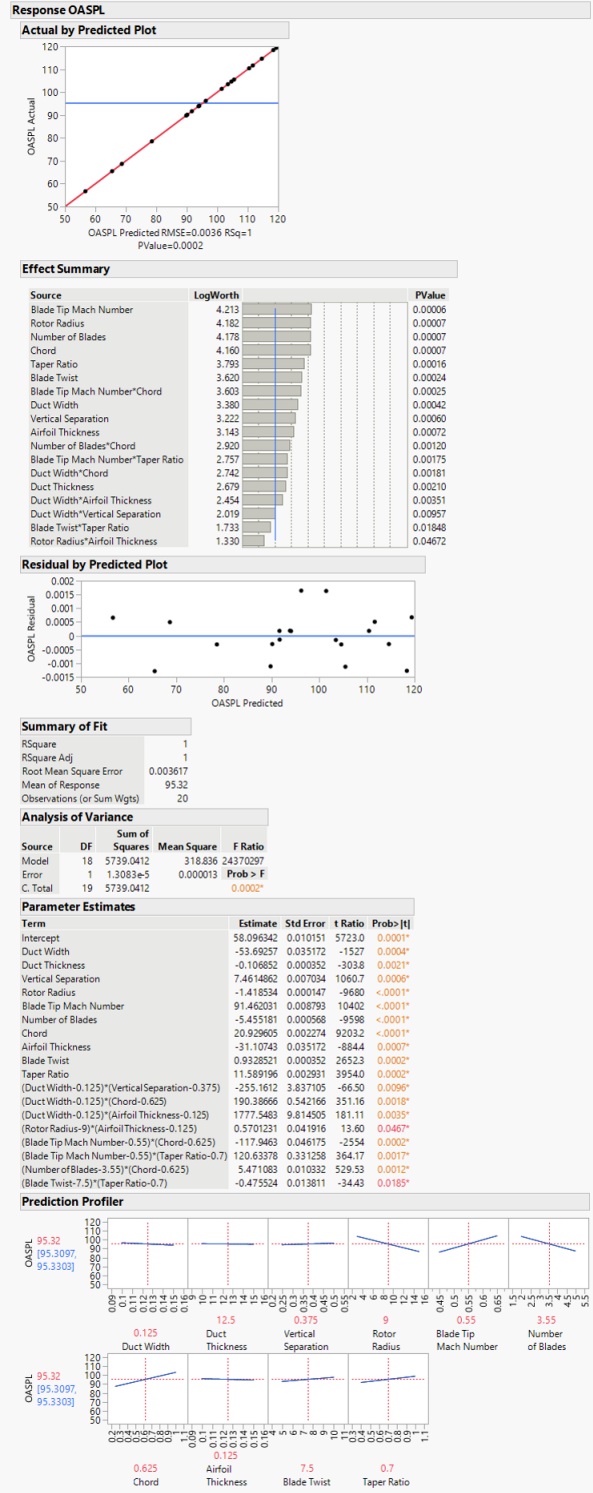

Figure 6.33: Stepwise regression model for *both* cases

6.3.3 Best Fit Representative Models

The models seem to fit the data exceptionally well across all fit types with an R-squared value of .8 or higher. There does not seem to be any large outliers across any of the models. Influential parameters within the profilers for all the models show consistent impact to noise. This shows the consistency and the validity in the data.

For each of the configurations, the best fitting model is the stepwise regression model with an R-squared value of one. This means that the stepwise regression model is a perfect fit to the data and can accurately represent the configurations individually.

With the influential parameters within the profilers being very similar across each configurations, the equations show that they would be similar. This alludes to a model being able to represent the data across all three configurations.

$$
\begin{aligned}
OSAPL = {} & 46.56 + 5.08 * VerticalSeparation \\
& - 1.44 * RotorRadius \\
& + 102.75 * BladeTipMachNumber \\
& - 4.96 * NumberofBlades \\
& + 16.47 * Chord \\
& + -61.78 * AirfoilThickness \\
& + 1.09 * BladeTwist \\
& + 14.47 * TaperRatio \\
& + (VerticalSeparation - 0.375) * (Chord - 0.625) * 18.25 \\
& + (BladeTipMachNumber - 0.55) * (NumberofBlades - 3.5625) * 46.11 \\
& + (NumberofBlades - 3.56) * (Chord - 0.625) * 1.91s \\
& + (NumberofBlades - 3.5625) * (TaperRatio - 0.7) * 0.26 \\
& + (Chord - 0.625) * (BladeTwist - 7.5) * -3.36 \\
& + (BladeTwist - 7.5) * (TaperRatio - 0.7) * -4.26
\end{aligned}
\tag{6.1}
$$

$$
\begin{aligned}
OASPL \;=\;& 45.37 - 31.47 * DuctThickness \\
& + 0.29 * DuctWidth \\
& - 1.3032 * RotorRadius \\
& + 72.94 * BladeTipMachNumber \\
& - 1.06 * NumberofBlades \\
& + 17.497 * Chord \\
& - 0.067 * AirfoilThickness \\
& + 1.22 * BladeTwist \\
& + 7.24 * TaperRatio \\
& + (DuctWidth - 12.5) * (BladeTipMachNumber - 0.55) * 34.24 \\
& + (DuctWidth - 12.5) * (Chord - 0.625) * -33.86 \\
& + (DuctWidth - 12.5) * (TaperRatio - 0.7) * -0.5032 \\
& + (RotorRadius - 9) * (BladeTipMachNumber - 0.55) * -15.427 \\
& + (RotorRadius - 9) * (BladeTwist - 7.5) * 2.220 \\
& + (RotorRadius - 9) * (TaperRatio - 0.7) * 0.799 \\
& + (NumberofBlades - 3.55) * (Chord - 0.625) * 0.31 \\
& + (NumberofBlades - 3.55) * (TaperRatio - 0.7) * -50.63 \\
& + (AirfoilThickness - 0.125) * (TaperRatio - 0.7) * 3003.95
\end{aligned}
$$

$$
\begin{aligned}
OASPL \;=\; & 58.1 + -53.69 * DuctWidth \\
& + -0.11 * DuctThickness \\
& + 7.46 * VerticalSeparation \\
& + -1.42 * RotorRadius \\
& + 91.46 * BladeTipMachNumber \\
& + -5.46 * NumberofBlades \\
& + 20.93 * Chord \\
& + -31.11 * AirfoilThickness \\
& + 0.93 * BladeTwist \\
& + 11.59 * TaperRatio \\
& + (DuctWidth - 0.125) * (VerticalSeparation - 0.375) * -255.16 \\
& + (DuctWidth - 0.125) * (Chord - 0.625) * 190.39 \\
& + (DuctWidth - 0.125) * (AirfoilThickness - 0.125) * 1777.55 \\
& + (RotorRadius - 9) * (AirfoilThickness - 0.125) * 0.57 \\
& + (BladeTipMachNumber - 0.55) * (Chord - 0.625) * -117.95 \\
& + (BladeTipMachNumber - 0.55) * (TaperRatio - 0.7) * 120.63 \\
& + (NumberofBlades - 3.55) * (Chord - 0.625) * 5.47 \\
& + (BladeTwist - 7.5) * (TaperRatio - 0.7) * -0.48
\end{aligned}
$$

CHAPTER 7

SUMMARY AND CONCLUSIONS

While the design space of the types of vehicles has opened up, so has a literature gap of further information about them. This thesis researched the current and future state of urban air mobility in terms of acoustics in hopes to fulfill this gap. Reviewing the previously stated research questions displays the found results.

How is the configuration space for rotor noise analysis quantified? This question led to looking how to bound the run matrices for this experiment, which was done based on previous research, as well as the interests of the current UAM designers in the industry. When it comes to quantifying the outputs of these designs and configuration, in a way where it is consistent across the space, a noise metric was used to quantify the space into one specific number. OSAPL was used to capture the noise, as it has very little weighting in one direction or another on the spectrum or in terms of time of day or duration. Primarily, rotor noise was quantified by the influential parameters using JMP's bootstrap foresting partitioning. The portion displays the percent of significance to the overall output and therefore the quantification. This could be negative or positive influence it is not specified here. Within the prediction profiler for each of the representative models the significance is displayed further. This shows how influential each parameter is to the model and in what direction they are influential. The graph can display several kinds of significance, such as parabolic, linear, etc.

What are the most important parameters to consider when designing according to rotor noise? The run matrices were divided by the configuration parameters and the rotor specific design parameters. The OASPL outputs were put through the bootstrap foresting partitioning showing the important parameters to the systems. They displayed the rotor specific design parameters being much more influential in comparison to the configuration

parameters. The most significant driver of noise across all three configurations was shown to be blade tip Mach number, which confirms the physics of the systems, that speed drives noise. Chord length and rotor radius also show to be large drivers of noise across all three configurations. After the third parameters the parameters start to vary in influence across the systems.

How would the effect of parameters on different noise types be predicted? It was desired to have a process that would allow for the pinpointing of noise to the design parameters. This was done using PSU-WOPWOP to allow for the FWH equation to break down noise into thickness and loading noise. Then the noise was traced towards the parameters directly using JMP predictor screening (bootstrap partitioning) to discover significant drivers of noise. Spectrum analysis displayed thickness noise as a the major contributor to noise compared to loading noise. The influential parameters confirmed this further by showing that chord was within the top three significant drivers of noise. In order to predict this for future designs and work in a quick and efficient manner for the conceptual design stage, several kinds of models were made to fit data. It was shown that a stepwise regression model fits the data the best.

How would the interaction of architectural configurations and noise be predicted? The combination of the duct and coaxial cases into the *both* cases allows analysis of the configurations interacting. As shown through the influential parameter analysis, the configuration parameters do not seem to effect the noise significantly. Therefore the configuration does not play as much of importance as the rotor design itself. It seems that the rotor analyzed alone, will give a good sense of noise levels, but this was not compared to previous semi-empirical models.

Looking at the hypotheses of the thesis further shows what has been proven or disproven. The first hypothesis stated that if design and configuration parameters can be related to noise outputs by controlled detailed modeling, a simplified model can be built to replicate it. There were clear trends across the influential parameters, that remained con-

sistent through each of the model profilers. This showed consistency and validity of the experiment. It also showed that a model could be generated well enough to replicate this process. The stepwise regression model showed a good fit of the data.

While the second hypothesis sates that, if noise trends are apparent across various configurations, then acoustic considerations can be accounted for in the conceptual design stage across the UAM design space of interest. While trends are apparent, they were only apparent for rotor designs and not the configuration space. This may not hold true across a larger design space with more complex, or combined configurations, but within the space specified here it proved to be effective. Since the trends were apparent, it is concluded that acoustic considerations can be accounted for early on in the design stage.

Overall, non-traditional configurations can provide many benefits in terms of performance and acoustics. This study gave insight into the source noise generation of various configurations that are still being researched. Some of these configurations can be layered on top of each other for a combination effect, but analysis showed that rotor analysis outside of configuration is more significant. Trends showed to be apparent across the configurations and a representative model fit the data well enough to be used for future designs. This will allow designers to account for noise considerations early on in the conceptual design stage.

7.1 Future Work

This study did not utilize a sensitivity study for CFD meshing since each configuration would require one for the most accurate results. It would be recommended to do one because it allows for improved convergence and resolution. PSU-WOPWOP was used for this research, but many different acoustic solvers exist, such as CAA which would be more accurate, with the drawback of being more computationally expensive to use. If there was a desire for a higher degree of accuracy, CAA would be recommended.

This study only account for the effects of the parameters listed in 2.1 through 2.3 and

their associated ranges. These ranges are directly linked to the outputs that were shown in the results. The order can change dramatically with a different set of ranges. This research can be expanded to include a larger range of parameters, using this same methodology. Other parameters have been shown to effect noise of rotorcraft vehicles that could be included. This would mean expanding the Mach number and, therefore, include noise phenomena within the supersonic regime. Therefore, more analysis could be done looking at BVI and HSI in more detail. A future study could potentially include more, less, or different, parameters to show effects.

There was only one case within the DOEs in which all the parameters matched across the configurations. It would be recommended to have more cases in which the parameters matched in order to draw more conclusive results.

The FAA has not yet created standards for these UAM vehicles, therefore certain parameters were chosen in order to help control the experiment. Only hover was analyzed in this thesis. It would be important in the future to discover the noise within take off and landing of these vehicles because of the proximity to the people it would be effecting. This would add more variables into the experiment. If the FAA were to determine standard approach and departure procedures for these UAM vehicles then that could be followed. To look at a single overall noise value, OASPL was used. This metric has it's own weightings. Since the FAA has not yet provided a metric, it would be interesting to see how the results change in terms of metrics.

This study was done with the intent to create a process to overall lessen noise and, therefore, human annoyance. Pyschoacoustics, the study of human perception of noise, is a growing field. Humans may perceive noise that is annoying much louder than it actually is. To be able to track a human perception of noise across configurations would allow designers to send more time on the aspects of the design that generate the annoyance. This allows for more targeted and productive design. A pyschoacoustic study would require a variety of human subjects to rank their annoyances and have that traced back to the sources

of noise. There are many other noise metrics that attempt to do this in more simplified ways which could be utilized, such as A-weighting or Community Tolerance Level (CTL). Ultimately, the human response is what will allow these vehicles to be implemented into daily life.

REFERENCES

[1] N. L. Schatzman, "Aerodynamics and aeroacoustic sources of a coaxial rotor," *NASA*, 2018.

[2] Nickolas Polaczyk, Enzo Trombino, Peng Wei, Mihaela Mitici, "A Review of Current Technology and Research in Urban On-Demand Air Mobility Applications," *Vertical Flight Society Autonomous VTOL Technical Meeting and Electric VTOL Symposium*, 2019.

[3] F. Reuter, *The Volocopter Flies!* NASA ODM Workshop, 2016.

[4] Michael Doty, *Overview of Unmanned Aircraft System (UAS) Noise Research at NASA Langley Research Center*, Aircraft Noise and Emissions Reduction Symposium, 2017.

[5] Krish Ahuja, "Helicopter Noise and its Control," Class Notes, 2019.

[6] D. Zeddies, "Local Acoustic Particle Motion Guides Sound-Source Localization Behavior in the Plainfin Midshipman Fish," *Journal of Experimental Biology*, pp. 152–160, 2012.

[7] K. Van den Abeele, J. Ramboer, G. Ghorbaniasl and C. Lacor, *Computational Fluid Dynamics: Numerical Solution of the Linearized Euler Equations Using Compact Schemes*. ICCFD, 2006.

[8] T. Yang, "Study of active rotor control for in-plane rotor noise reduction," PhD thesis, The Pennsylvania State University, 2016.

[9] Jack Marte, Donald Kurtz, "A Review of Aerodynamic Noise From Propellers, Rotors, and Lift Fans," *NASA*, 1970.

[10] Yongjie Shi, Teng Li, Xiang He, Linghua Dong, Guohua Xu, "Helicopter Rotor Thickness Noise Control Using Unsteady Force Excitation," *Applied Sciences*, 2019.

[11] K. Brentner and F. Farassat, "Modeling Aerodynamically Generated Sound of Helicopter Rotors," *The Pennsylvania State University*, 2003.

[12] W. Villafana, "Rotorcraft Noise Abatement Procedures Development," Master's thesis, Pennsylvania State University, 2016.

[13] J. Zentichko, "Acoustics of Ducted Rotor," Master's thesis, Pennsylvania State University, 2010.

[14] Daniel Wachpress, Todd Quackenbush, "Impact of Rotor Design on Coaxial Rotor Performance, Wake Geometry and Noise," *American Helicopter Society*, 2006.

[15] Leighton Myers, Wook Rhee, Dennis McLaughlin, "Aeroacoustics of Vertical Lift Ducted Rotors," *AIAA*, 2009.

[16] R. Pegg, "A summary and evaluation of semi-empirical methods for the prediction of helicopter rotor noise," *NASA*, 1979.

[17] R. Arndt and D. Borgman, "Noise Radiation from Helicopter Rotors Operating at High Tip Mach Number," *American Helicopter Society*, 1970.

[18] Ollerhead and M.V. Lowson, "Studies of Helicopter Rotor Noise," *USA AVLABS Tech*, 1969.

[19] S.E. Wright, "Discrete Radiation from rotating Periodic Sources," *Journal of Sound and Vibration*, vol. 17, pp. 437–498, 1971.

[20] F. Farassat, "Thickness Noise of Helicopter Rotors at High Tip Speeds," *AIAA*, 1975.

[21] L.T. Filotas, "Vortex Induced Helicopter Blade Loads and Noise," *Journal of Sound and Vibration*, vol. 27, pp. 387–398, 1973.

[22] V. Blandeau, "Broadband Noise Due to Rotor- Wake/Rotor Interaction in Contra-Rotating Open Rotors," *AIAA*, vol. 48, 2010.

[23] Kyle Collins, Lakshmi Sankar, "Application of Low and High Fidelity Simulation Tools to Helicopter Rotor Blade Optimization," *American Helicopter Society*, 2009.

[24] C. Hennes, L. Lopes, J. Shirey, J. Erwin, and K. S. Brentner, *PSU-WOPWOP 3.3 User's Guide*. NASA Langley, 2009.

[25] K.S. Brentner and F. Farassat, "Analytical Comparison of the Acoustic Analogy and Kirchoff Formlation for Moving Surfaces," *AIAA*, 1998.

[26] F. Farassat, M. Myers, "Extension of Kirchoff's Formula to Radiation from Moving Surfaces," *NASA*, 1987.

[27] Kenneth Brentner, *Rotor Noise Modeling*, 5th Transformative Vertical Flight Workshop, 2018.

[28] Tim Colonius, Sanjiva Lele, "Computational Aeroacoustics: Progress on Nonlinear Problems of Sound Generation," *Progress in Aerospace Sciences*, 2004.

[29] Unknown, "Fast Forwarding to a Future of On Demand Urban Air Transportation," *Uber Elevate*, 2016.

[30] *Uber Elevate*, website, https://www.uber.com/us/en/elevate/, 2019.

[31] James Baeder, Judith Gallman, Yung Yu, "A Computational Study of Aeroacoustics of Rotors in Hover," *American Helicopter Society*, 1993.

[32] David Robinson, *Replay Gain a Proposed Standard*, website, `http://replaygain.hydrogenad.io/proposal/equal_loudness.html`, 2019.

[33] R. Bennett and K. Pearsons, "Handbook of Aircraft Noise Metrics," *NASA*, 1981.

[34] Andrew Christian, Randolph Cabell, "Initial Investigation into the Psychoacoustic Properties of Small Unmanned Aerial System Noise," *NASA*, 2017.

[35] Nastasja von Conta, "Managing UAS Noise Footprint," *Altiscope*, 2018.

[36] Dimitri Mavris, "Design of Experiments for Practical Applications in Modeling and Simulation and Analysis: Introduction to Response Surface Methods," Class Notes, 2017.

[37] Tom Donnelly, *Creating and Analyzing Definitive Screening Designs*, JMP, 2013.

[38] *JMP Statiscal Discovery: Predictor Screening*, website, https://www.jmp.com/support/help/14-2/predictor-screening.shtml, 2019.

[39] Marcel Proust, "Modeling and Multivariate Methods," *JMP*, 2010.

[40] Santiago Balestrini-Robinson, `https://github.com/OpenVSP/OpenVSP/blob/master/src/python_api/api.py`.

[41] A. Akturk and C. Camci, "Tip clearance investigation of a ducted fan used in vtol unmanned aerial vehicles-part 1:baseline experiments and computational validation," *ASME, Journal of Turbomachinery*, 2014.

[42] *Creating Interfaces*, https://documentation.thesteveportal.plm.automation.siemens.com/starccmplus

[43] Alistair Field, "How to split and prepare domains for a rotating body simulation," *CD-Adapco*, 2017.

[44] J. Cornelius, "Efficient CFD Approaches for Coaxial Rotor Simulations," Master's thesis.

[45] Axel Kiekr, *Best Practices for Direct Noise Calculations*, website, Article Number: 12236, 2018.

[46] C. A. Wagner, T. Huttl, and P. Sagaut, *Large-Eddy Simulation for Acoustics*. Cambridge University Press, 2007.

[47] *Theory:Turbulence:Scale-Resolving Simulations:Detached Eddy Simulation (DES)*, website, `https://documentation.thesteveportal.plm.automation.siemens.com/starccmplus_latest_en/index.html#page/STARCCMP`, 2019.

Appendices

Please email me with any questions at shuelsman102@gmail.com